Contents

1 Geophysica flights

The following figures show measurements of chemical species along the flight paths of the Geophysica aircraft on 13 flights between 17 January and 10 March 2010. All flights started from Kiruna (Sweden) and probed the stratospheric polar vortex and surf zone. The supplement shows only a selection of the measured species and leaves out several of the long-lived tracers which show basically the same behaviour as N_2O and CH_4.

Results of the sensitivity runs are shown as colored lines for the species ClO, O_3 and NO_y. The figures for N_2O and CH_4 show only results for the reference run.

Additionally, the flight path and several parameters along the flight paths that are helpful for interpretation of the measurements are shown, including pressure, temperature and solar zenith angle.

Flight parameters	
Figure 1	Flight path
Figure 2	Pressure
Figure 3	Temperature
Figure 4	Solar zenith angle
Figure 5	Potential temperature
Figure 6	Equivalent latitude
Species	
Figure 7	ClO
Figure 8	O_3
Figure 9	N_2O
Figure 10	CH_4

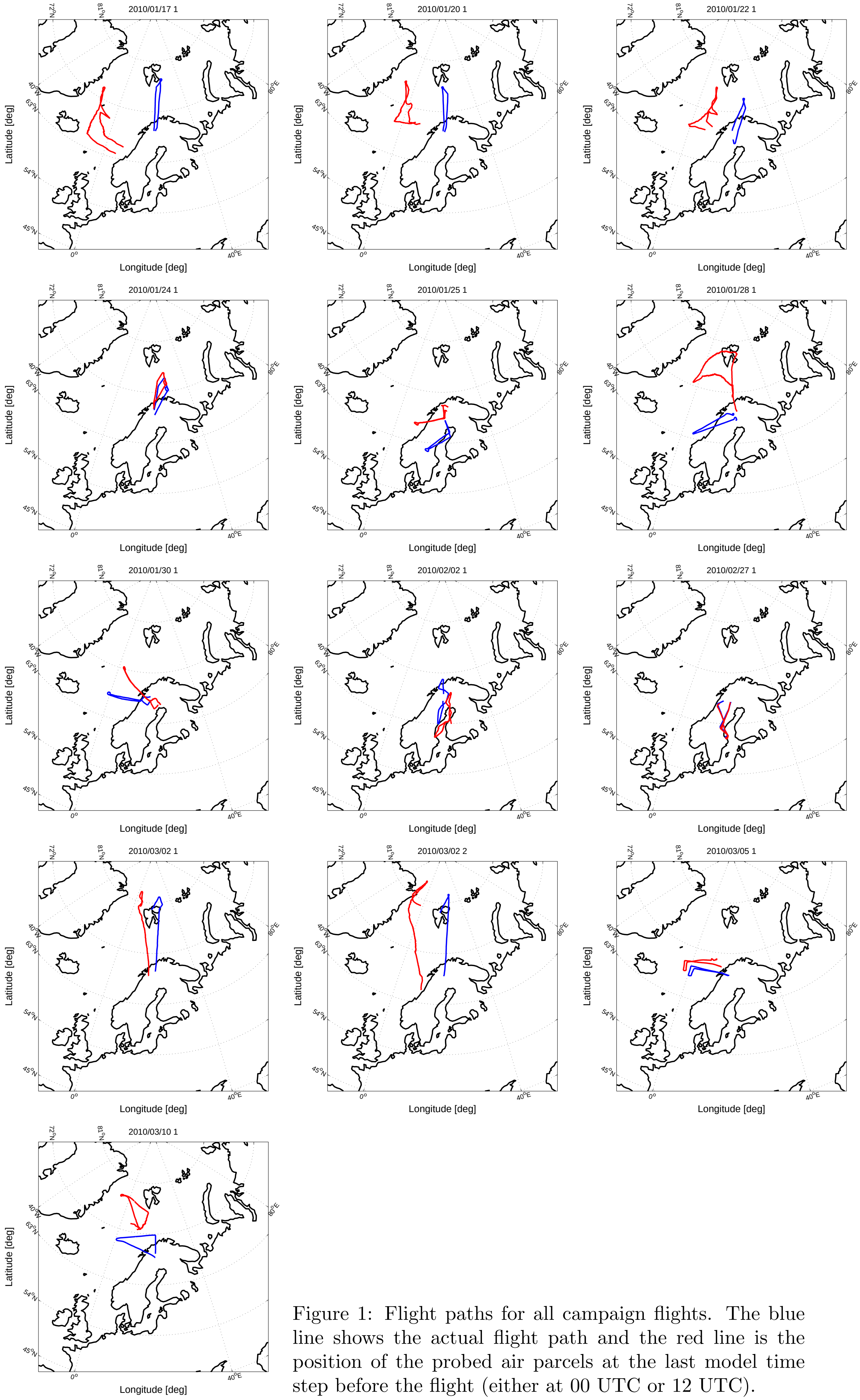

Figure 1: Flight paths for all campaign flights. The blue line shows the actual flight path and the red line is the position of the probed air parcels at the last model time step before the flight (either at 00 UTC or 12 UTC).

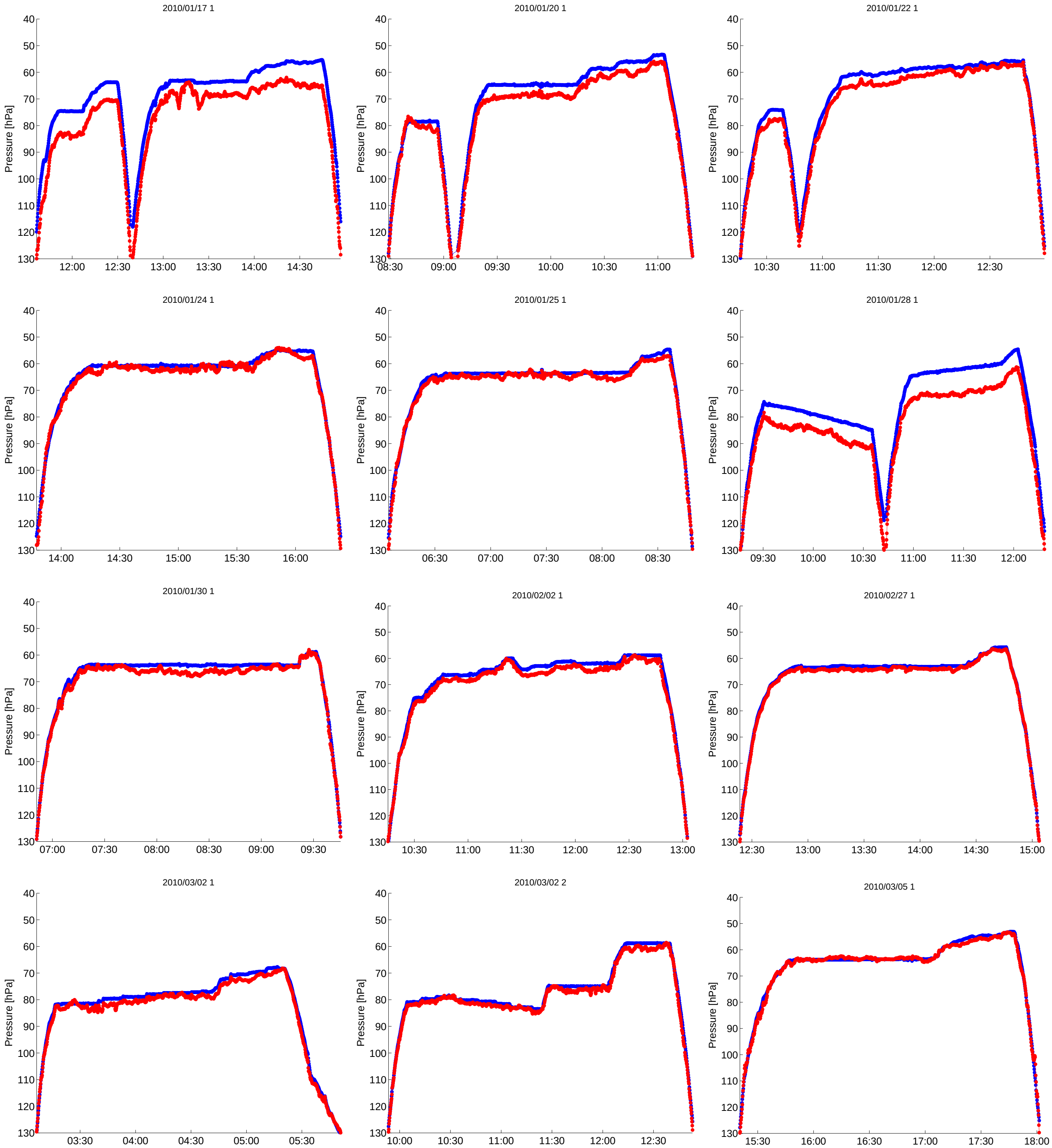

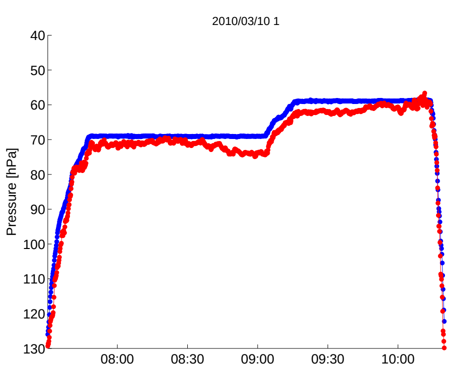

Figure 2: Pressure as a function of flight time (UTC). The blue line shows the pressure along the actual flight path (from Geophysica measurements) and the red line shows the pressure on the position of the probed air parcels at the last model time step before the flight (from the ERA Interim reanalysis, either at 00 h UTC or 12 h UTC).

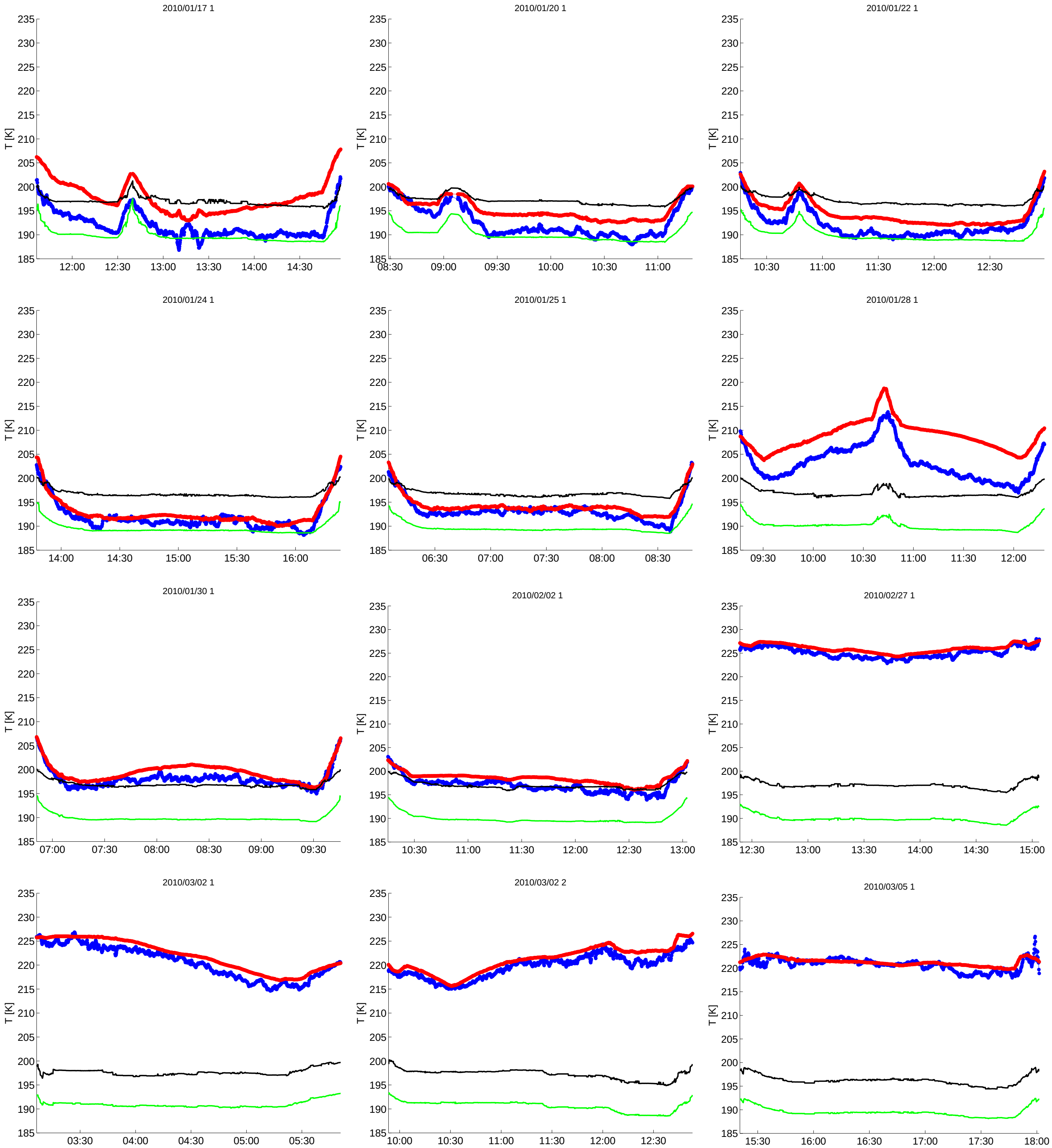

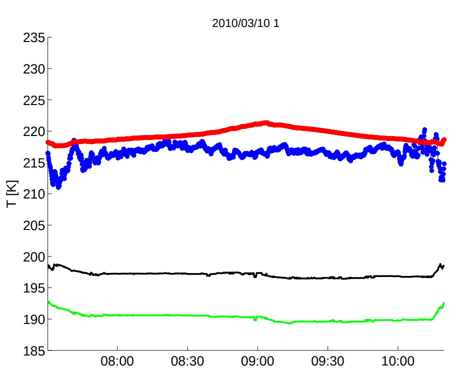

Figure 3: Temperature as a function of flight time (UTC). The blue line shows the temperature along the actual flight path (from Geophysica measurements) and the red line shows the temperature on the position of the probed air parcels at the last model time step before the flight (from the ERA Interim reanalysis, either at 00 h UTC or 12 h UTC). The thin black and green lines show the NAT and ice formation temperatures along the flight path.

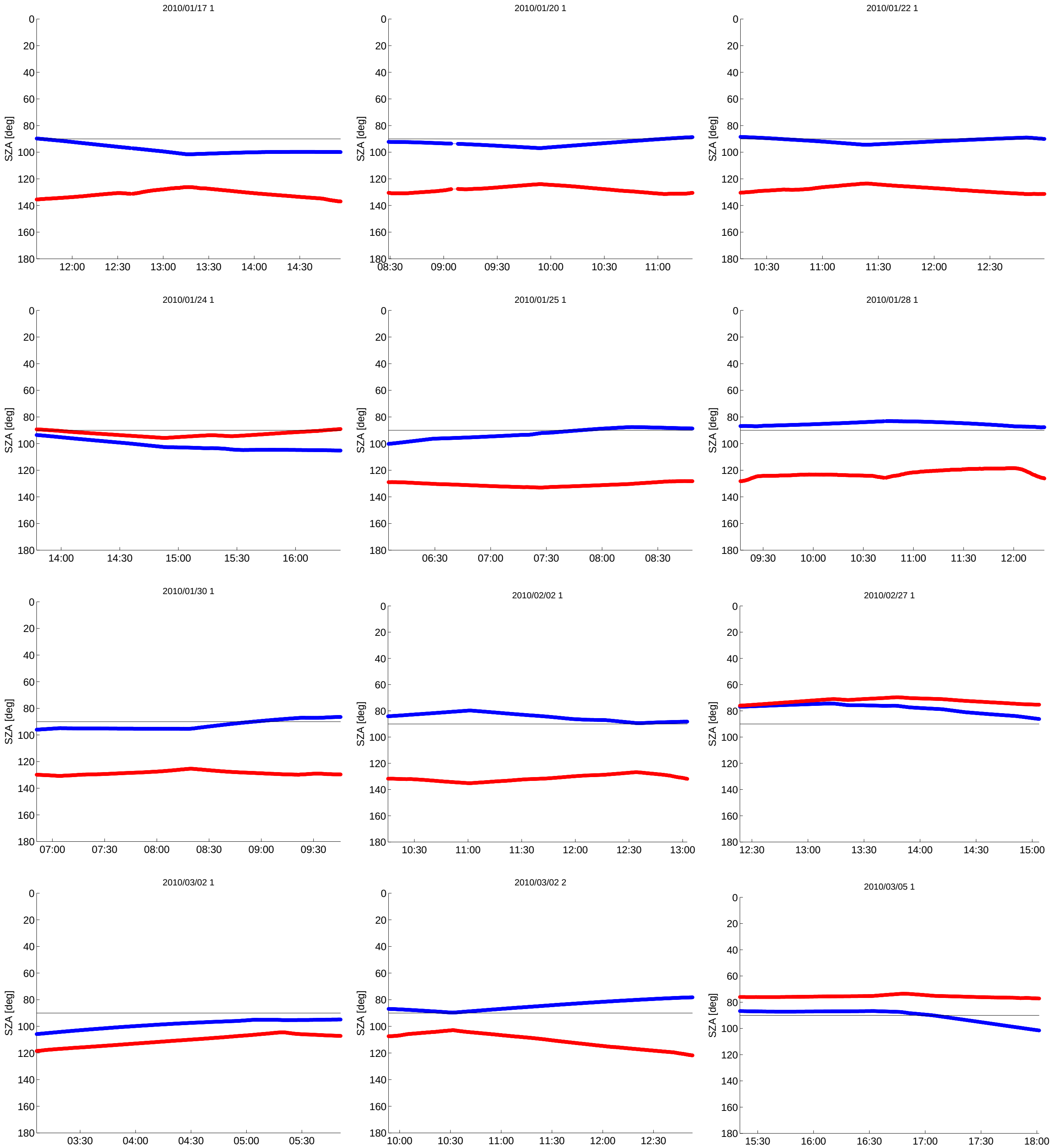

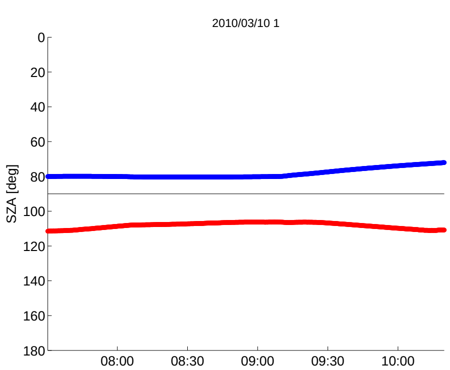

Figure 4: Solar zenith angle as a function of flight time (UTC). The blue line shows the solar zenith angle along the actual flight path and the red line shows the solar zenith angle on the position of the probed air parcels at the last model time step before the flight (either at 00 h UTC or 12 h UTC). The black line divides night and day.

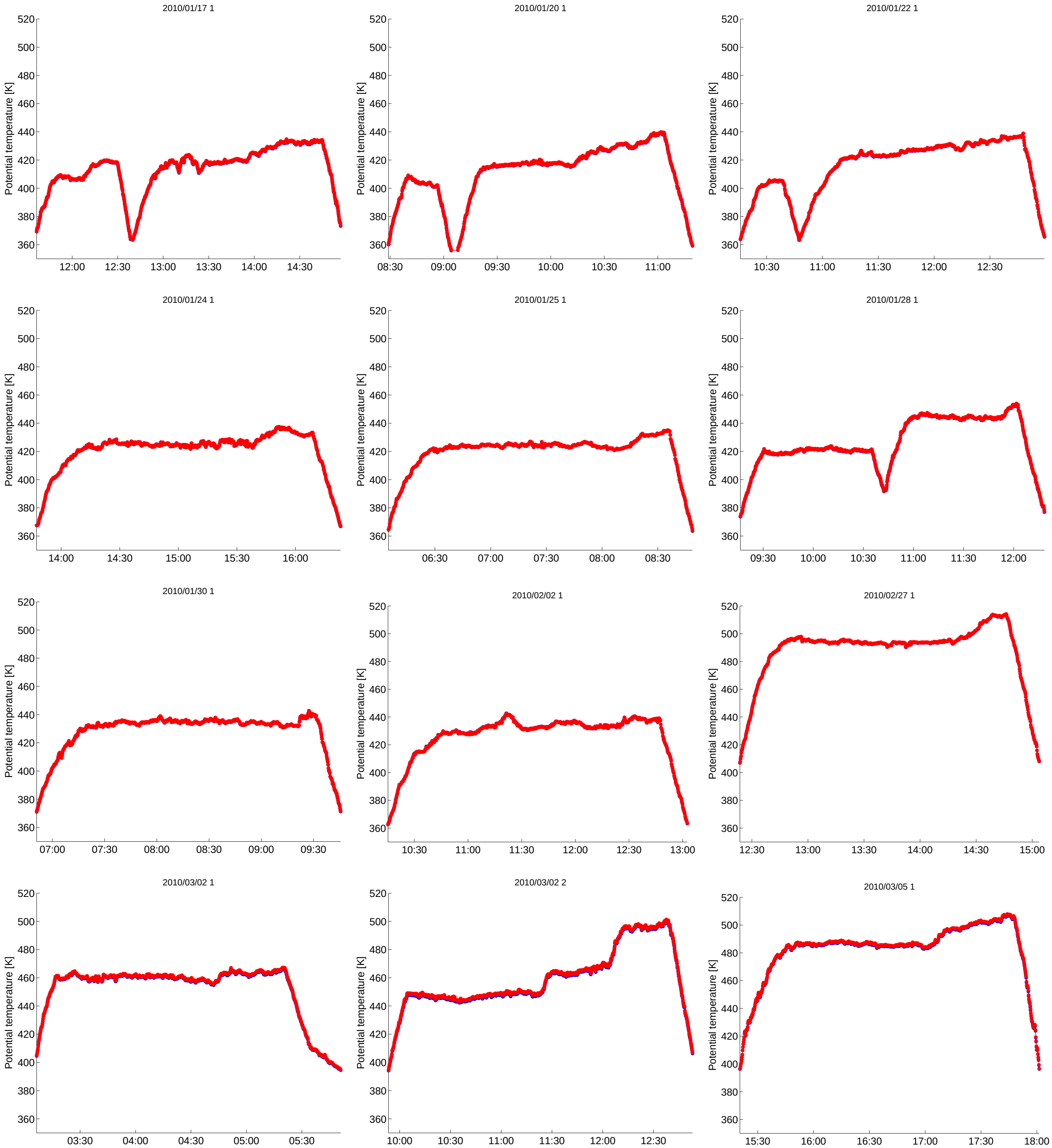

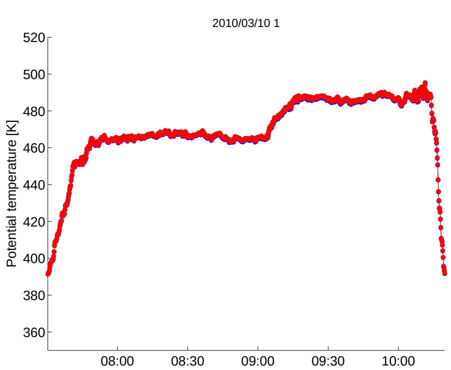

Figure 5: Potential temperature as a function of flight time (UTC). The blue line shows the potential temperature along the actual flight path (from Geophysica measurements) and the red line shows the potential temperature on the position of the probed air parcels at the last model time step before the flight (from the ERA Interim reanalysis, either at 00 h UTC or 12 h UTC).

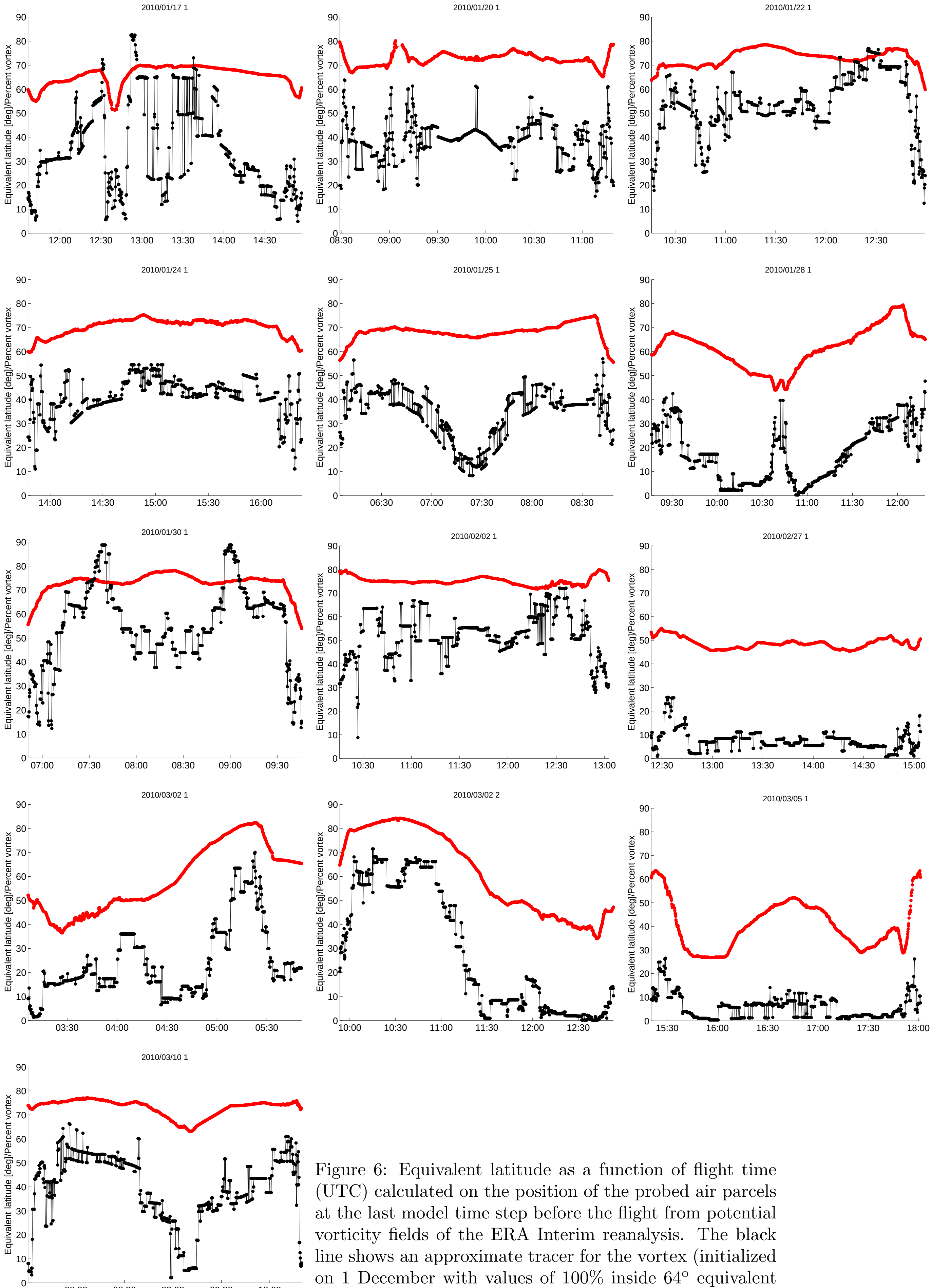

Figure 6: Equivalent latitude as a function of flight time (UTC) calculated on the position of the probed air parcels at the last model time step before the flight from potential vorticity fields of the ERA Interim reanalysis. The black line shows an approximate tracer for the vortex (initialized on 1 December with values of 100% inside 64° equivalent latitude and 0% elsewhere).

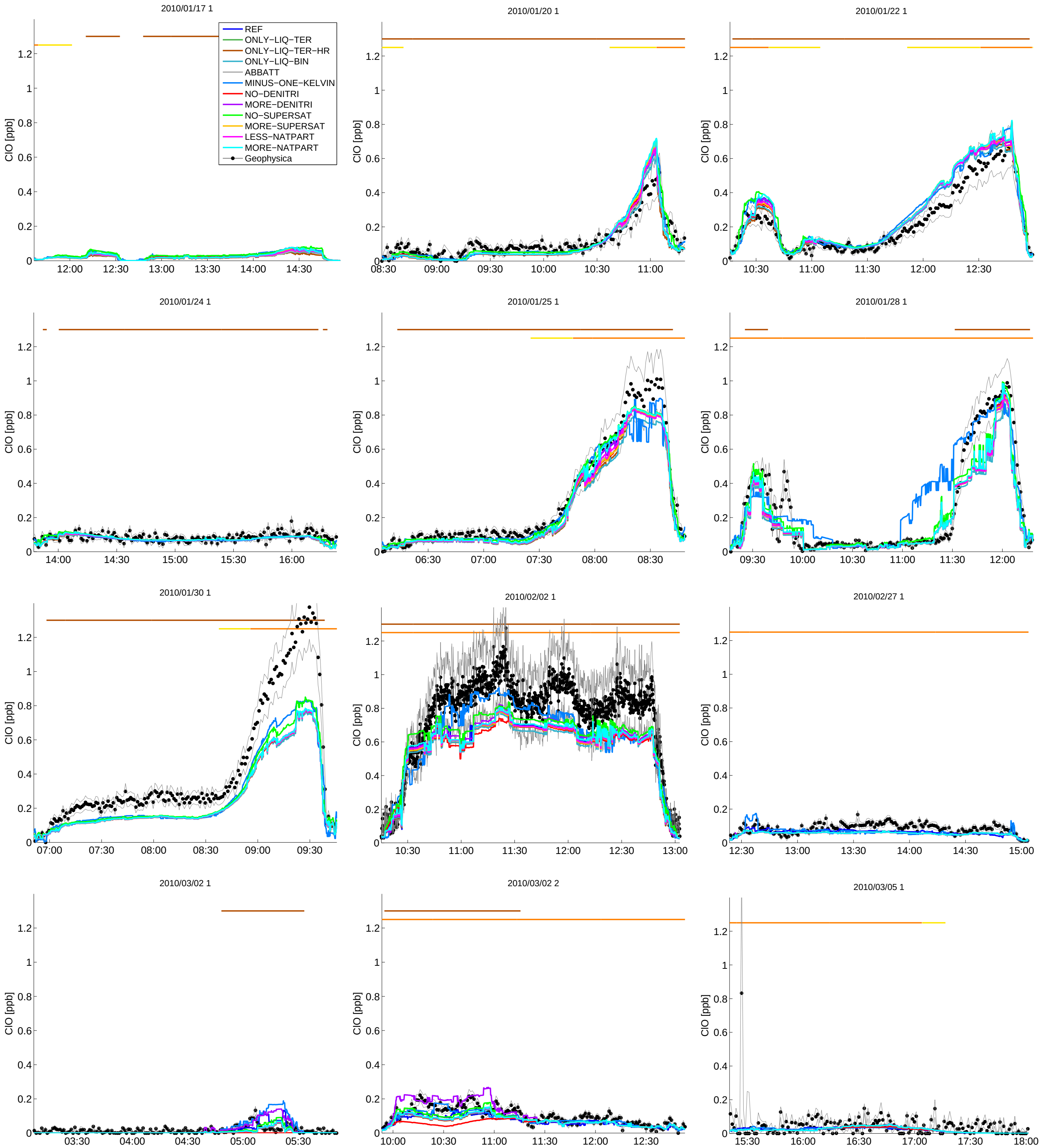

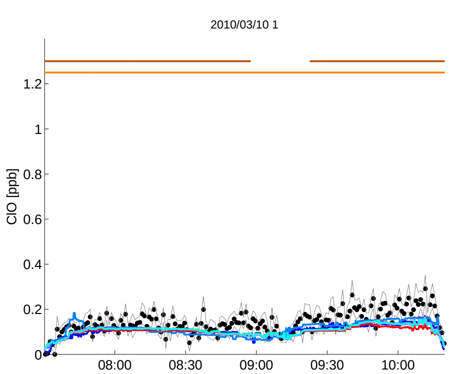

Figure 7: ClO as a function of flight time (UTC) from measurements of the HALOX instrument (black dots) onboard the Geophysica compared to modeled values of the reference run and all sensitivity runs (colored lines, color code in the first figure). Grey lines show uncertainties (accuracy and standard error). The brown line at the top indicates measurements inside the vortex (68.5° equivalent latitude). The yellow and orange lines show solar zenith angles below 92.5° (twilight) and 90° (day), respectively.

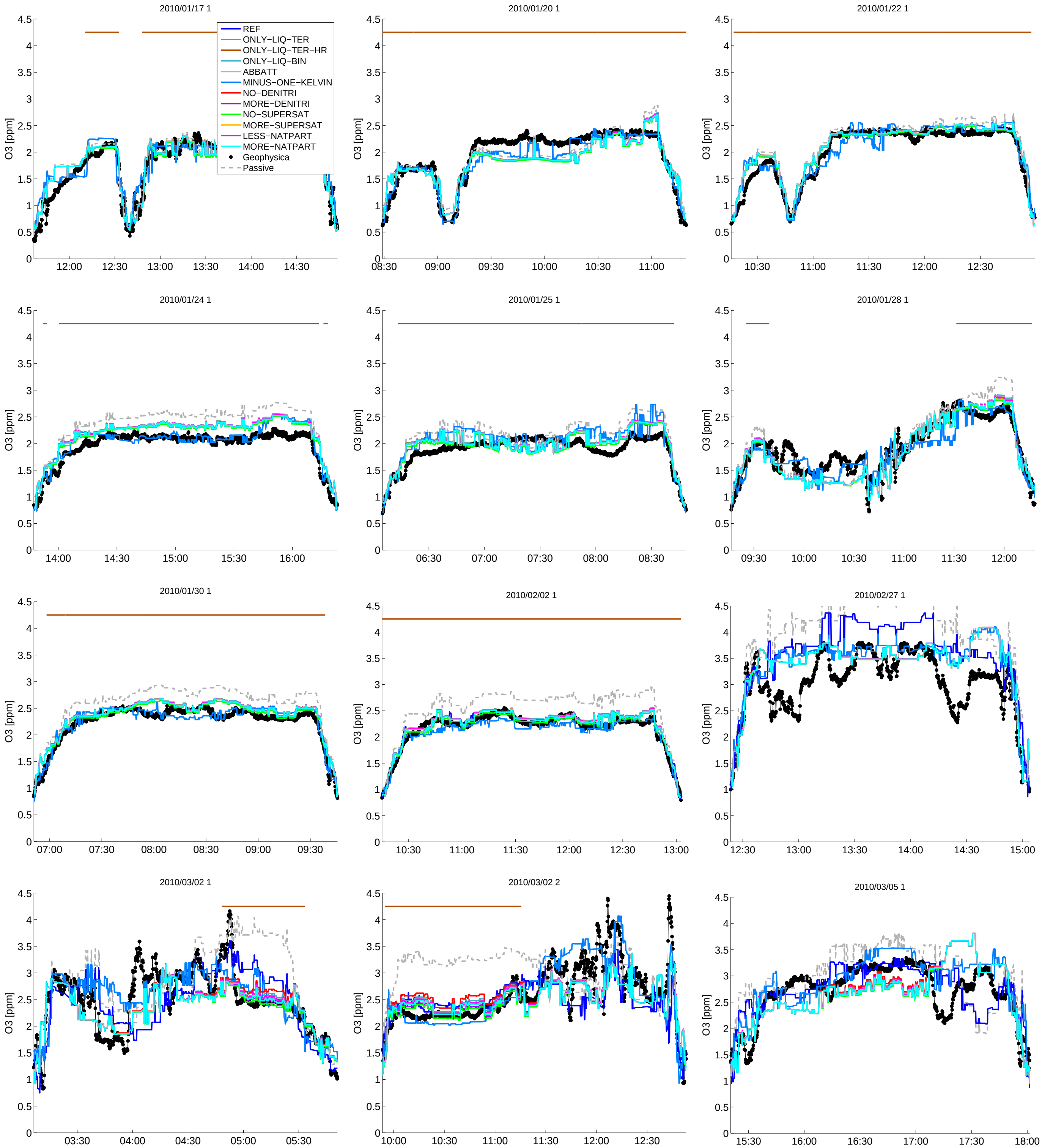

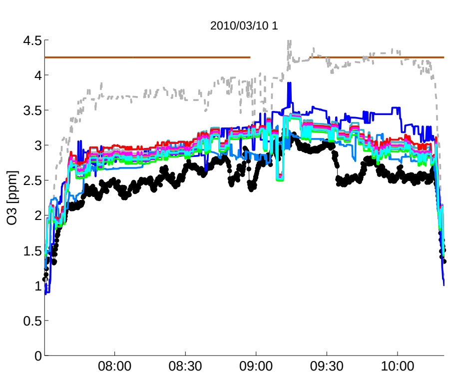

Figure 8: Ozone as a function of flight time (UTC) from measurements of the FOZAN instrument (black dots) onboard the Geophysica compared to modeled values of the reference run and all sensitivity runs (colored lines, color code in the first figure). The dashed grey line shows the passive ozone tracer. The brown line at the top indicates measurements inside the vortex (68.5° equivalent latitude).

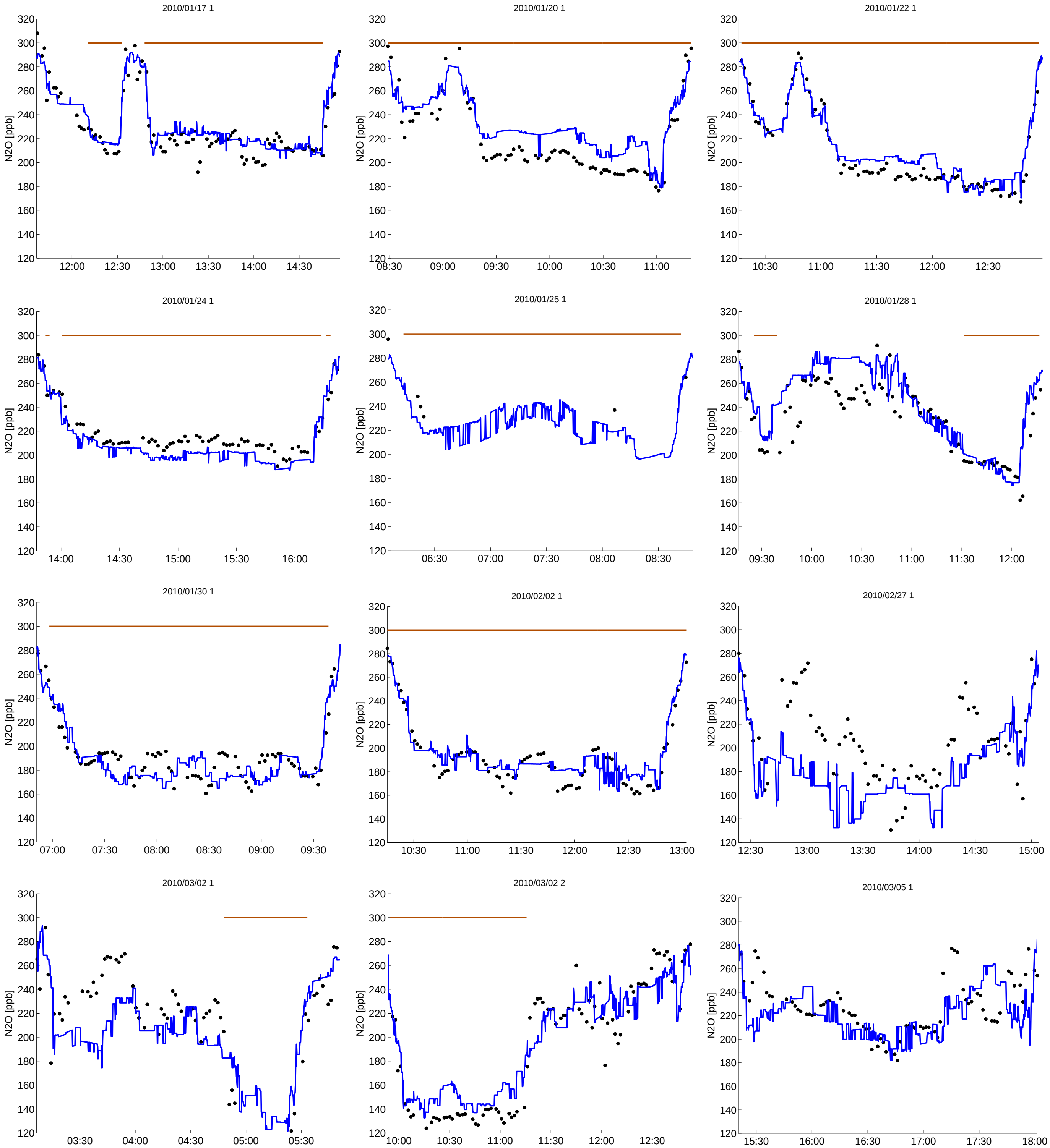

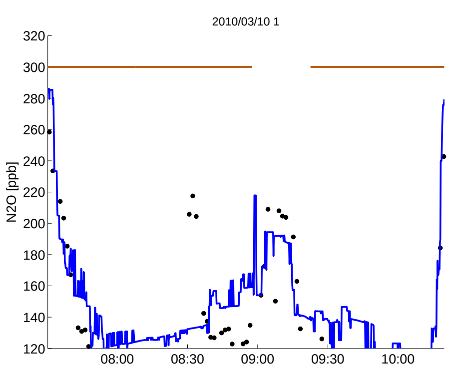

Figure 9: N_2O as a function of flight time (UTC) from measurements of the HAGAR instrument (black dots) onboard the Geophysica compared to modeled values of the reference run (blue line). The brown line at the top indicates measurements inside the vortex (68.5^o equivalent latitude).

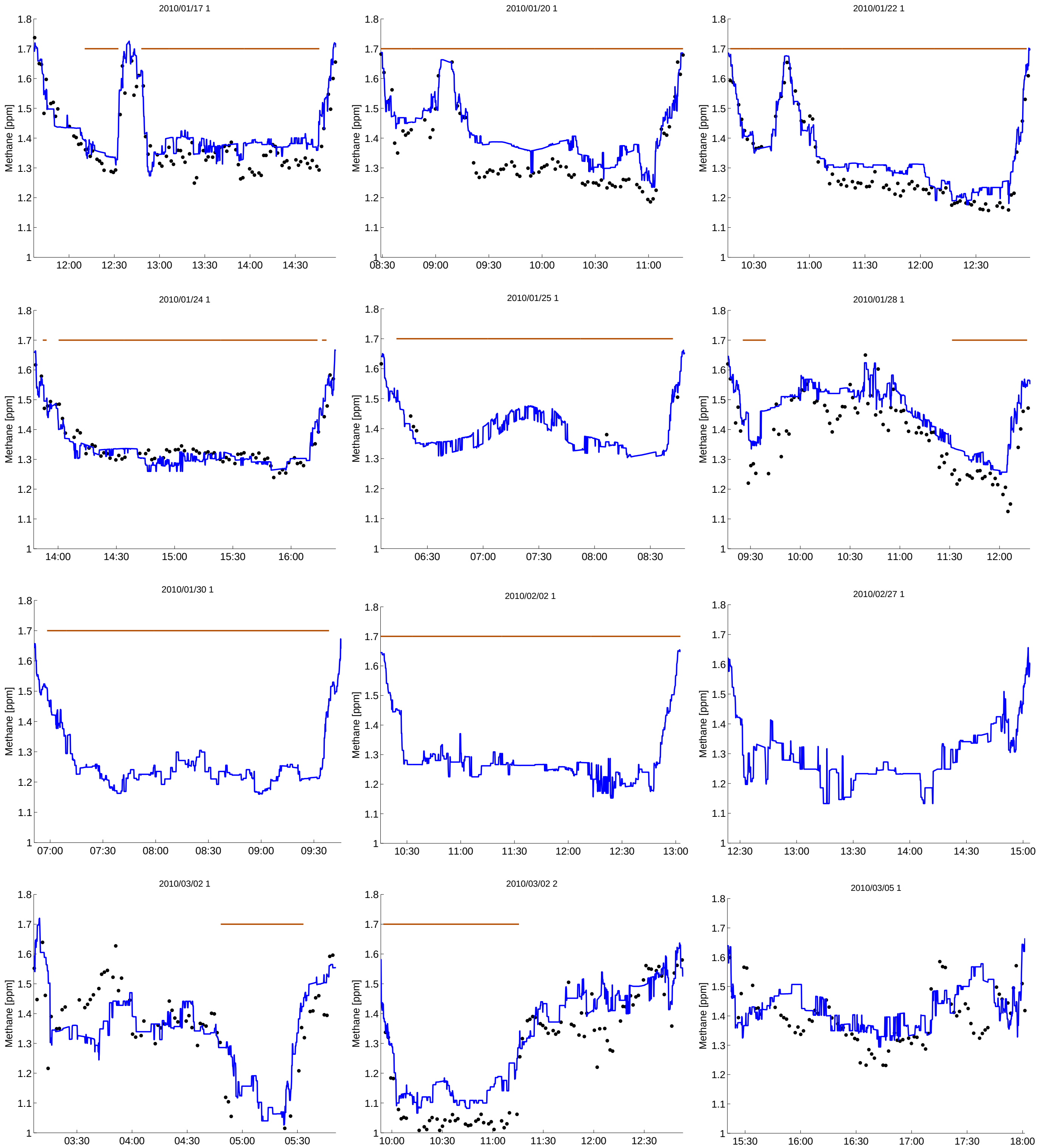

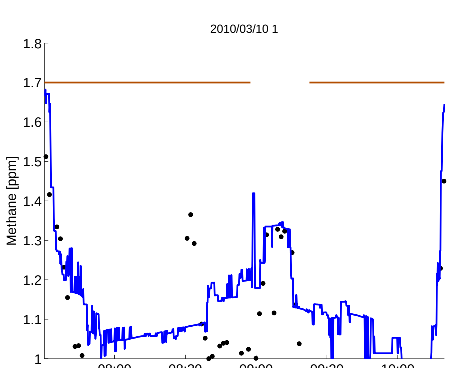

Figure 10: CH_4 as a function of flight time (UTC) from measurements of the HAGAR instrument (black dots) onboard the Geophysica compared to modeled values of the reference run (blue line). The brown line at the top indicates measurements inside the vortex (68.5° equivalent latitude).

2 Ozone sondes

The next figures show measurements of ozone sondes from the station Ny-Ålesund (12^o E, 79^o N) between January 2010 and March 2010.

Figures	
Figure 11	Temperature
Figure 12	Equivalent latitude
Figure 13	Ozone profiles

Subplots of each figure	
Number	Date
1	1.1
2	15.1
3	22.1
4	24.1
5	29.1
6	3.2
7	16.2
8	26.2
9	9.3
10	16.3

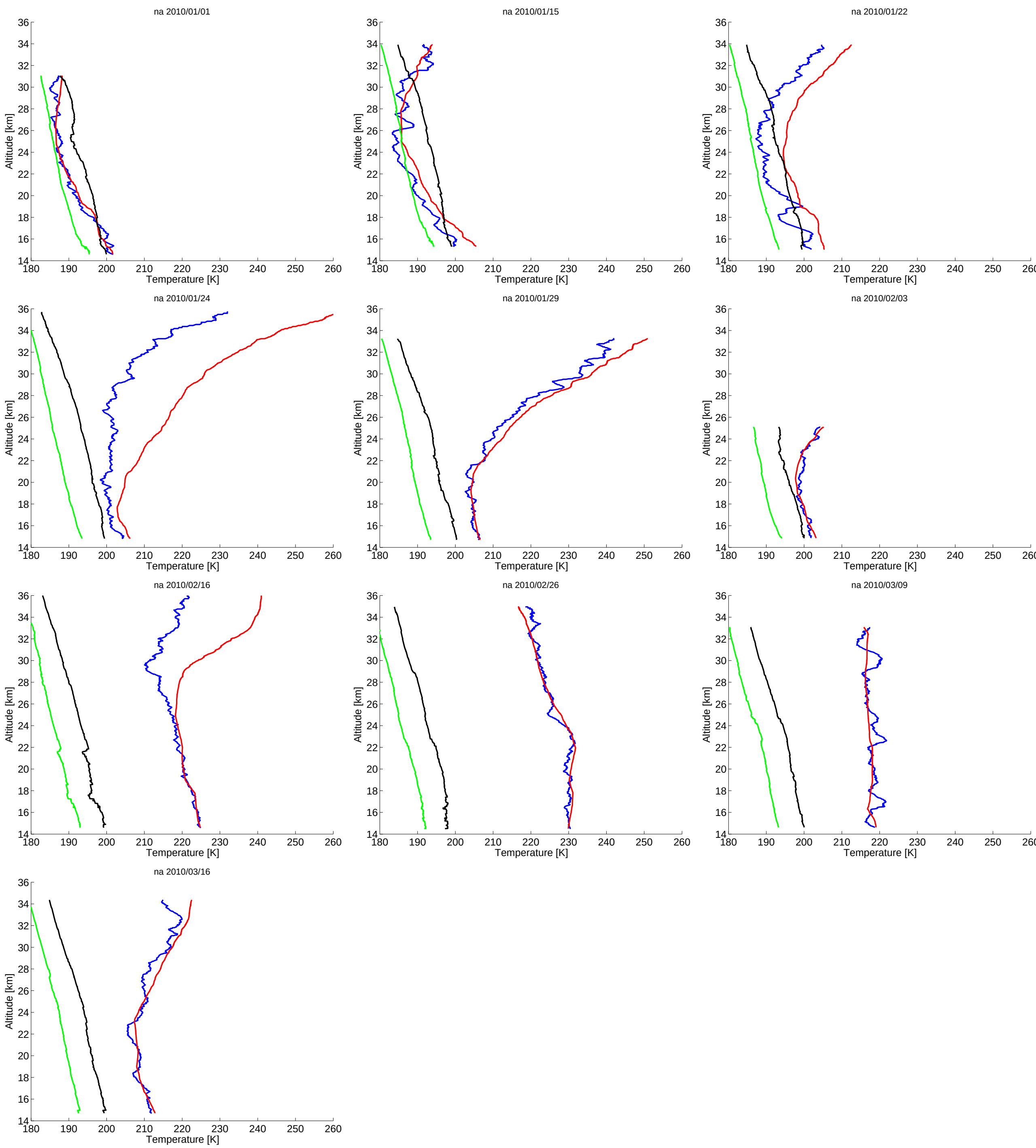

Figure 11: Temperature as a function of pressure altitude. The blue line shows the temperature measured by the sonde and the red line shows the temperature on the position of the probed air parcels at the last model time step before the flight (from the ERA Interim reanalysis). The thin black and green lines show the NAT and ice formation temperatures.

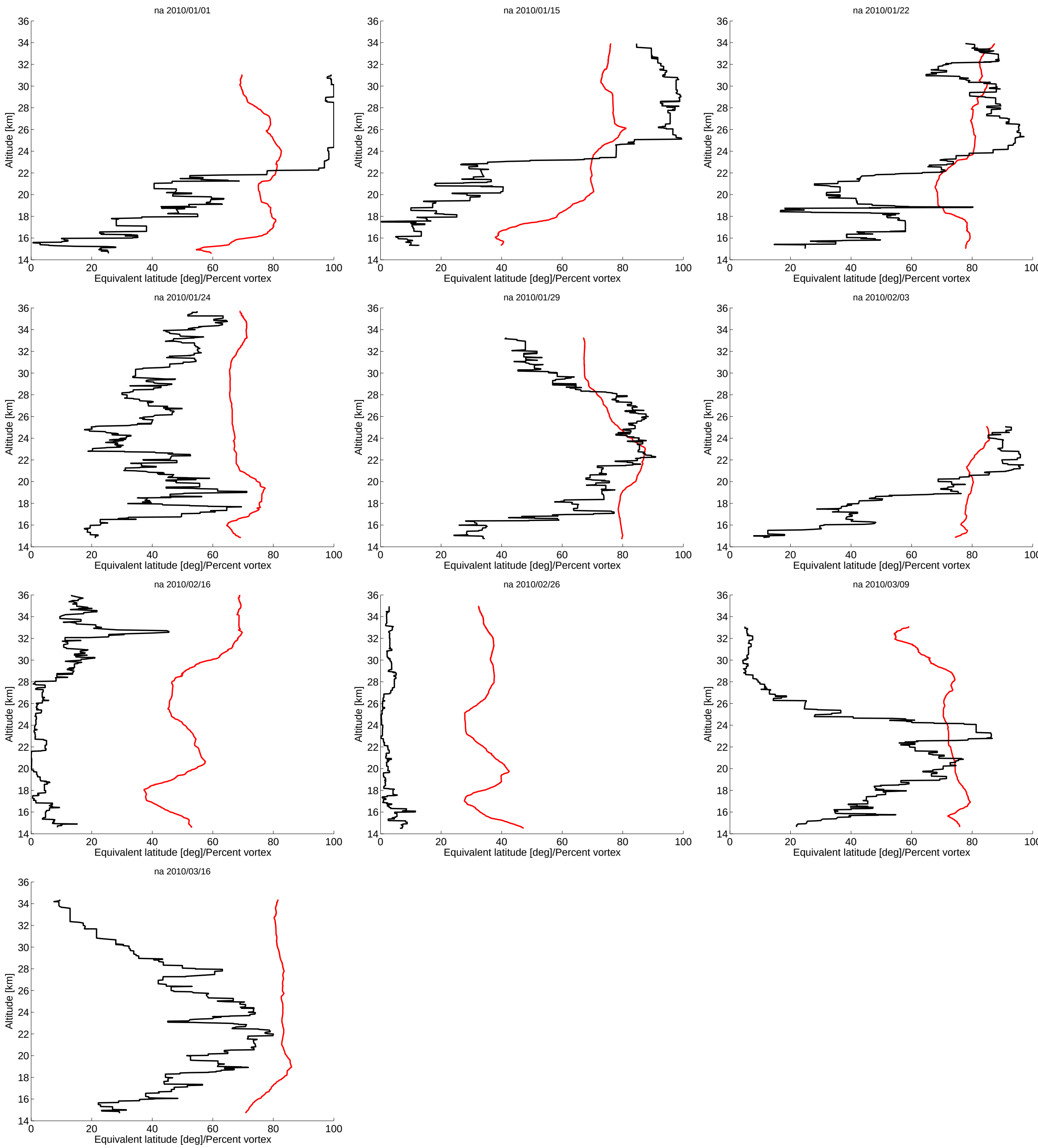

Figure 12: Equivalent latitude (red) as a function of pressure altitude calculated on the position of the probed air parcels at the last model time step before the flight from potential vorticity fields of the ERA Interim reanalysis. The black line shows an approximate tracer for the vortex (initialized on 1 December with values of 100 % inside 64° equivalent latitude and 0 % elsewhere).

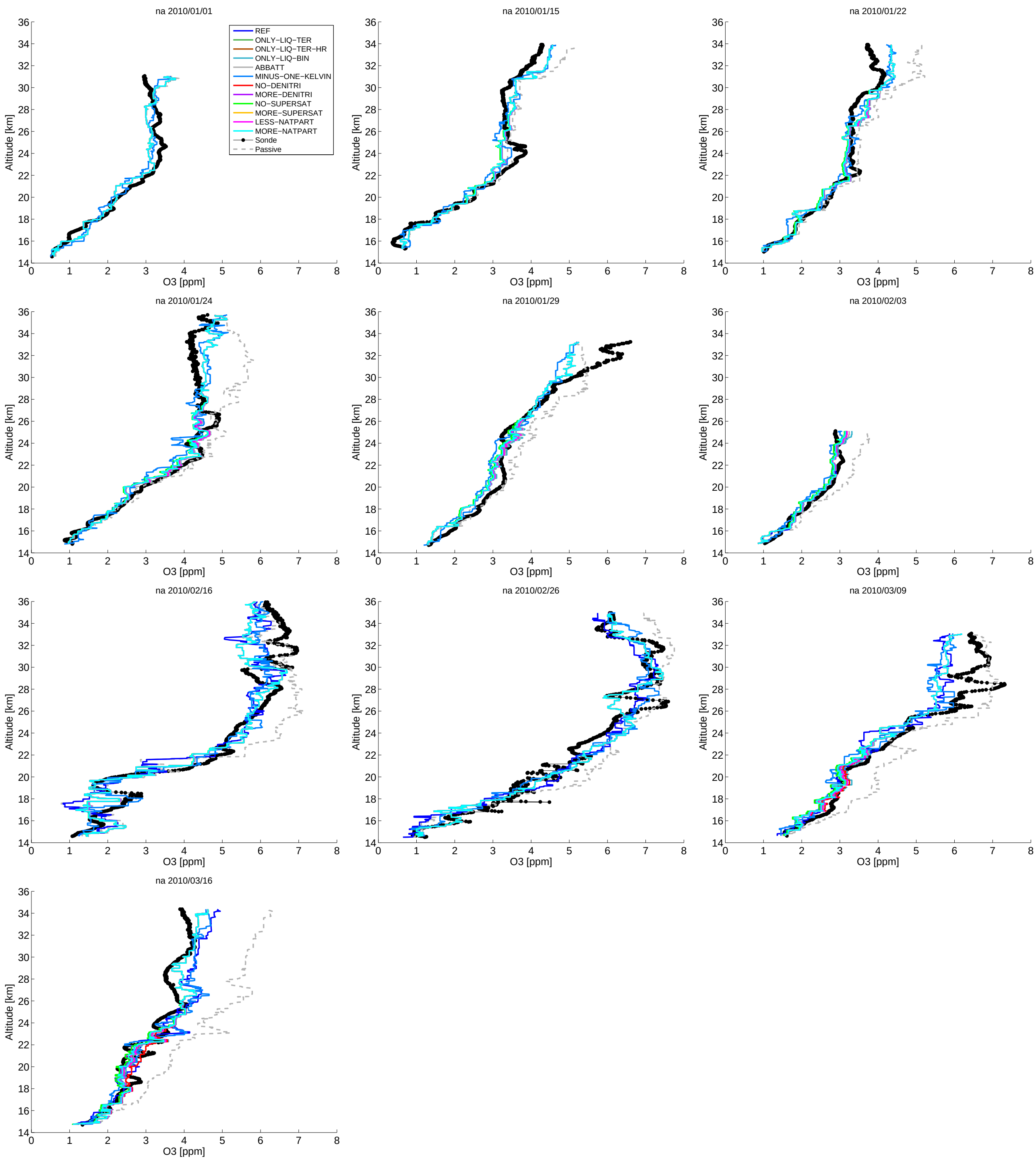

Figure 13: Measured ozone profiles (black dots) as a function of pressure altitude compared to modeled values of the reference run and all sensitivity runs (colored lines, color code in the first figure). The dashed grey line is the passive ozone profile.

3 ACE-FTS

The following figures show arbitrarily selected measurements of the ACE-FTS satellite instrument inside the vortex. Example profiles of H_2O, O_3, N_2O, CH_4, NO, NO_2, N_2O_5, NO_x, HNO_3, $ClONO_2$ and HCl are given for 5 January (56.8° N, 15.1° E), 25 January (65.2° N, 69.4° E) and 7 February (67.4° N, 29.3° E). Results of the sensitivity runs are shown as colored lines.

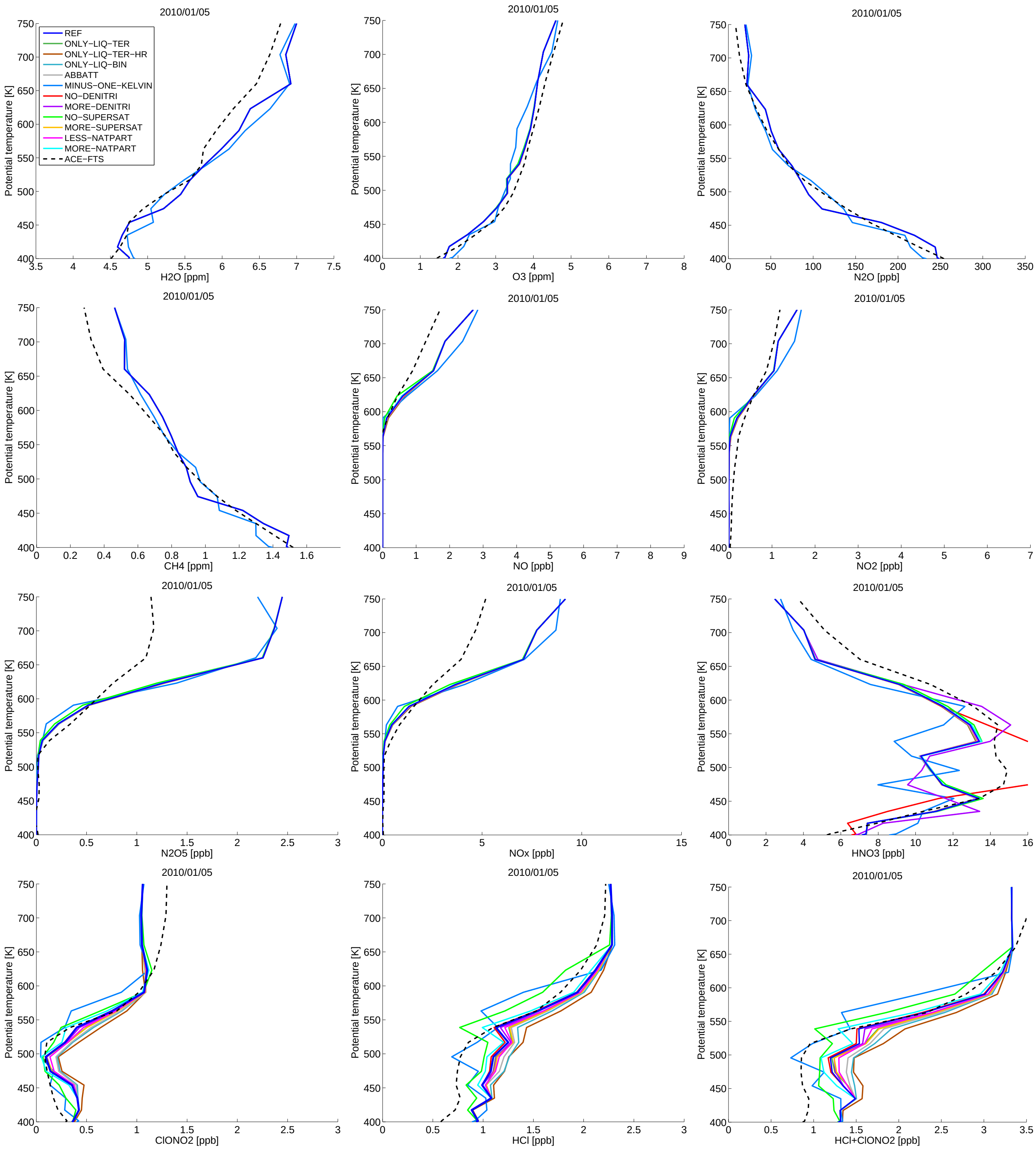

Figure 14: Example measurements of ACE-FTS on 5 January (56.8° N, 15.1° E) inside the vortex (black dashed lines). Profiles of H_2O, O_3, N_2O, CH_4, NO, NO_2, N_2O_5, $NO_x = NO + NO_2 + 2N_2O_5$, HNO_3 (gas phase), $ClONO_2$, HCl and $HCl + ClONO_2$. Colored lines show sensitivity runs (color code in the first figure).

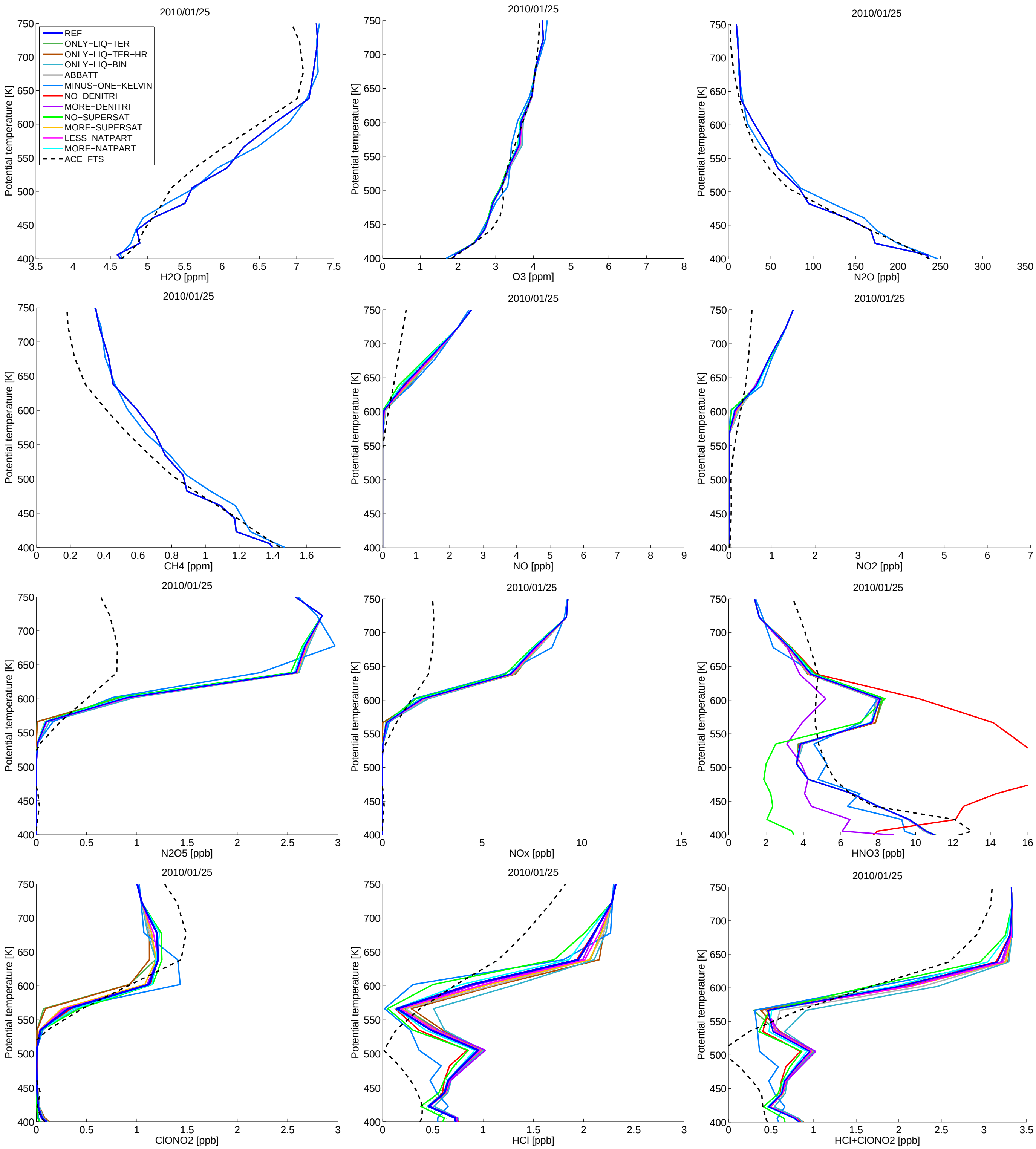

Figure 15: Example measurements of ACE-FTS on 25 January (65.2° N, 69.4° E)inside the vortex (black dashed lines). Profiles of H_2O, O_3, N_2O, CH_4, NO, NO_2, N_2O_5, $NO_x = NO + NO_2 + 2N_2O_5$, HNO_3 (gas phase), $ClONO_2$, HCl and $HCl + ClONO_2$. Colored lines show sensitivity runs (color code in the first figure).

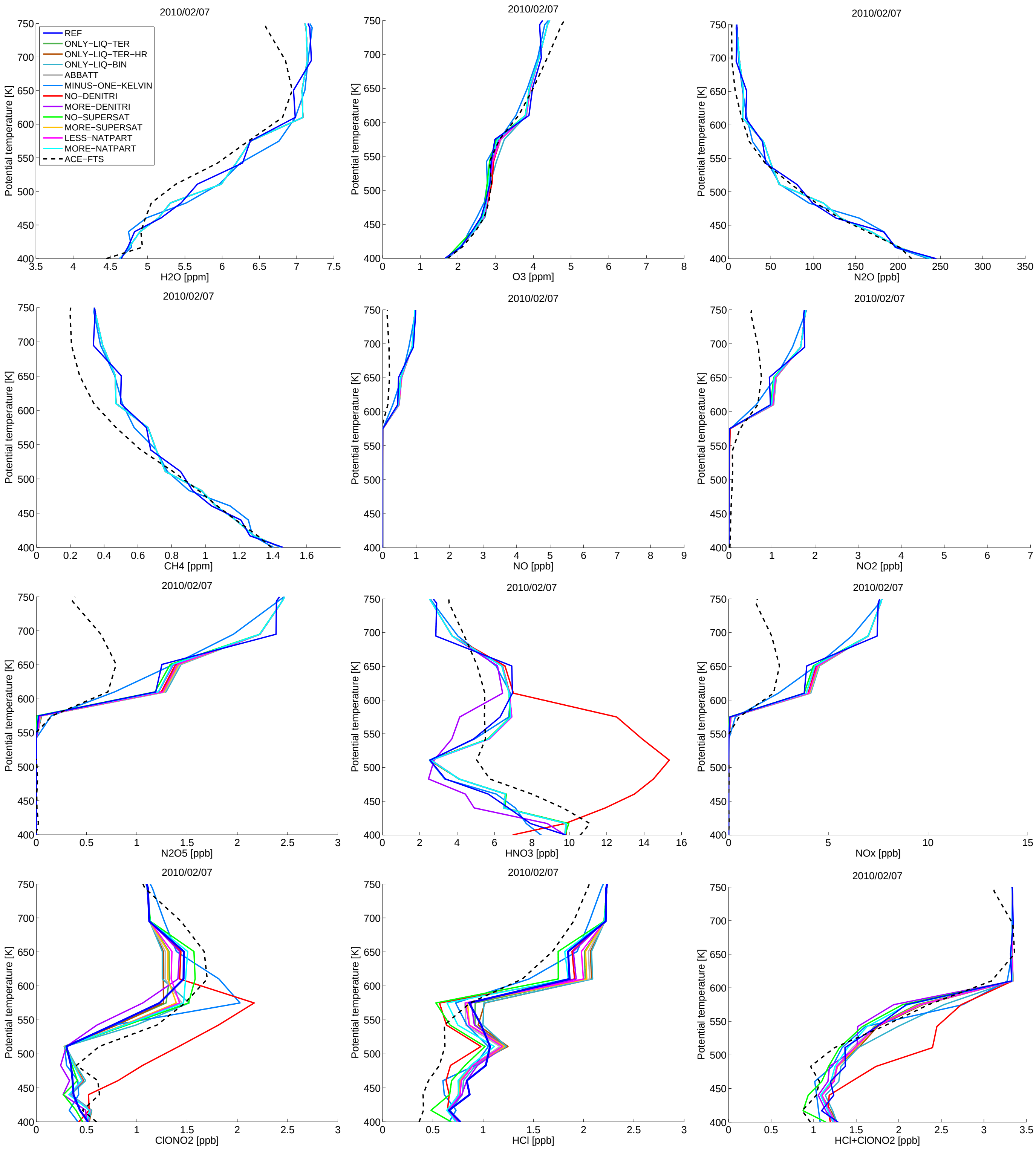

Figure 16: Example measurements of ACE-FTS on 7 February (67.4° N, 29.3° E) inside the vortex (black dashed lines). Profiles of H_2O, O_3, N_2O, CH_4, NO, NO_2, N_2O_5, $NO_x = NO + NO_2 + 2N_2O_5$, HNO_3 (gas phase), $ClONO_2$, HCl and $HCl + ClONO_2$. Colored lines show sensitivity runs (color code in the first figure).

4 MLS ClO comparisons with box model runs

For the next figures, backward trajectories starting at selected satellite measurements and ending at the time of the last model output before the measurement were calculated. Then, a chemical box model was initialized with the model data and the evolution of the species was calculated forward in time to obtain values to compare with the satellite measurements. Results are shown for the MLS layer at 46 hPa and 3 January, 17 January, 27 January and 13 February.

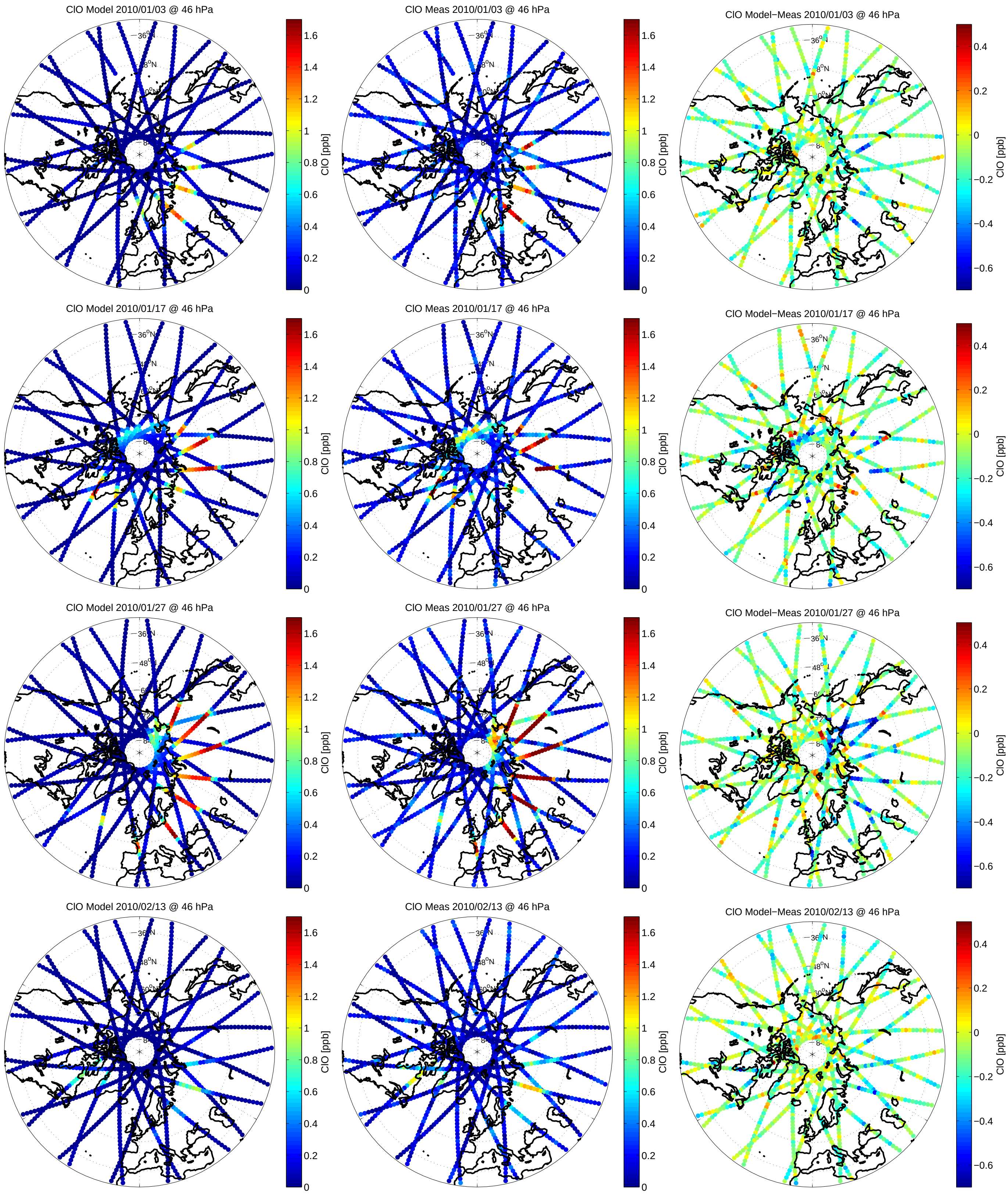

Figure 17: Modeled (left) and measured (middle) ClO mixing ratios at the MLS layer centered at 46 hPa along the satellite tracks. The rows show all measurements on 3 January, 17 January, 27 January and 13 February. The right column shows the differences. Backward trajectories starting at selected satellite measurements and ending at the time of the last model output before the measurement were calculated. Then, a chemical box model was initialized with the model data and the evolution of the species was calculated forward in time to obtain values to compare with the satellite measurements.

5 Vortex means

The next figures show modeled vortex means as a function of date and potential temperature averaged over all air parcels inside the vortex boundary according to the Nash criterion and over several hybrid coordinate (i.e. potential temperature) intervals equivalent to the vertical resolution of the model.

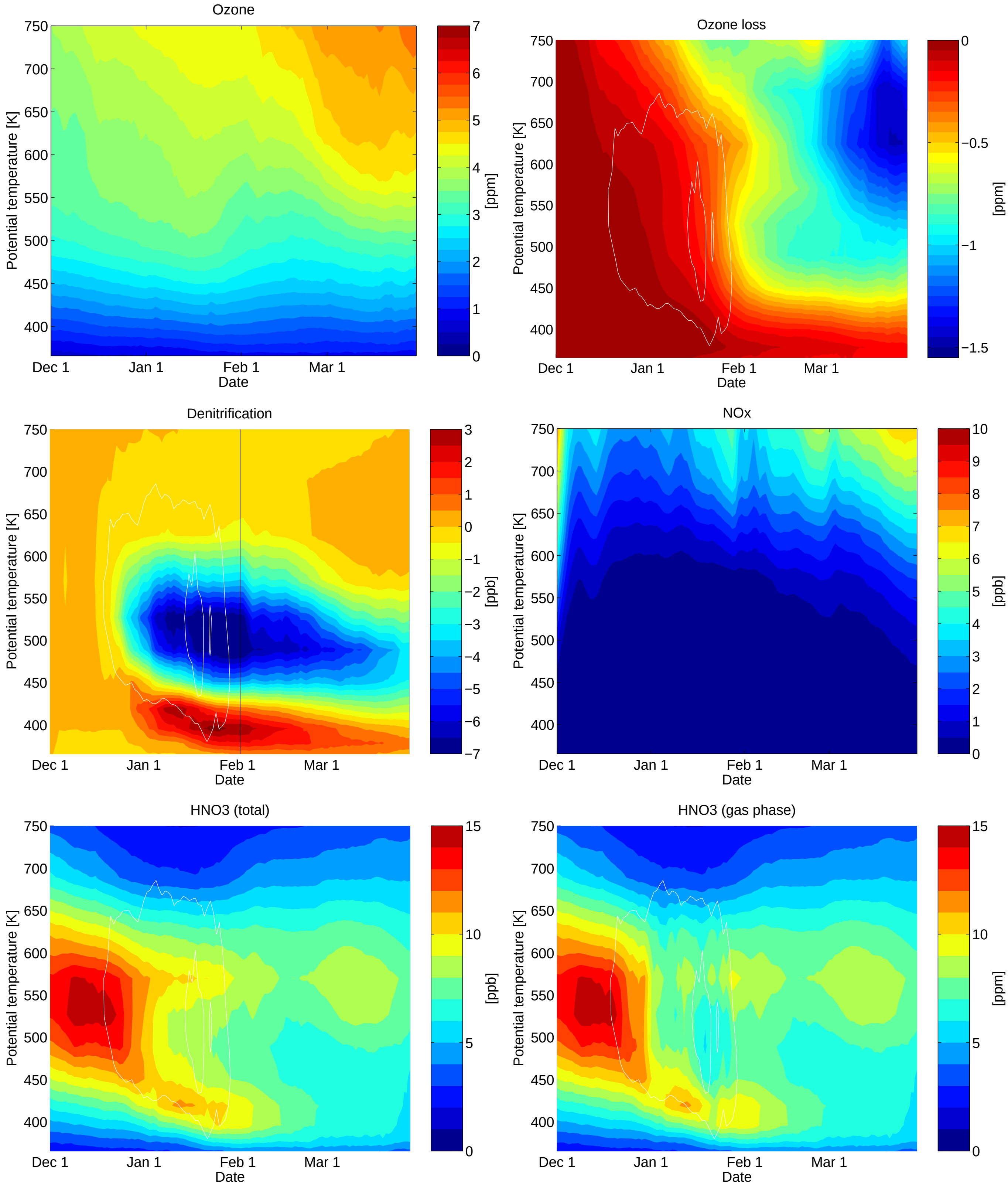

Figure 18: Vortex means as a function of model date and potential temperature inside the vortex boundary according to Nash. Ozone, ozone loss (difference of ozone to passive tracer), denitrification (difference of NO_y to passive tracer), NO_x, HNO_3 (total) and HNO_3 (gas phase). White lines show the time periods where the formation of NAT clouds (outer line) and ice clouds (inner line) was possible inside the vortex.

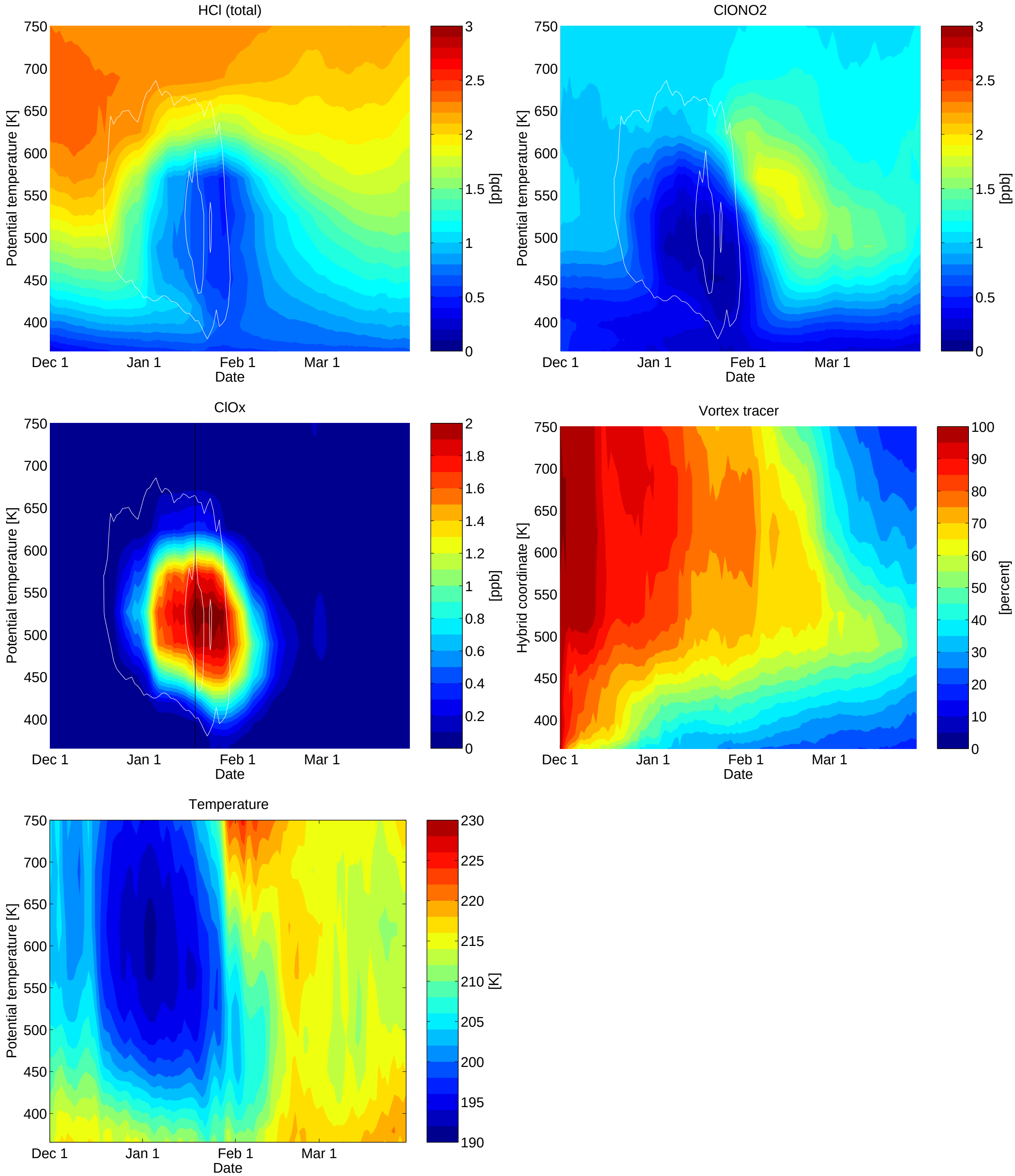

Figure 19: Vortex means as a function of model date and potential temperature inside the vortex boundary according to Nash. HCl, $ClONO_2$, ClO_x, vortex tracer, temperature. White lines show the time periods where the formation of NAT clouds (outer line) and ice clouds (inner line) was possible inside the vortex. One of the plots shows an approximate tracer for the vortex (initialized on 1 December with values of 100 % inside 64° equivalent latitude and 0 % elsewhere).

6 Comparison of sensitivity runs to reference run

The next figures show comparisons of the vortex means of the sensitivity runs and the reference run as a function of date and potential temperature.

Sensitivity run	
Figure 20	ONLY-LIQ-TER
Figure 22	ONLY-LIQ-TER-HR
Figure 24	ONLY-LIQ-BIN
Figure 26	ABBATT
Figure 28	MINUS-ONE-KELVIN
Figure 30	NO-DENITRI
Figure 32	MORE-DENITRI
Figure 34	NO-SUPERSAT
Figure 36	MORE-SUPERSAT
Figure 38	LESS-NATPART
Figure 40	MORE-NATPART

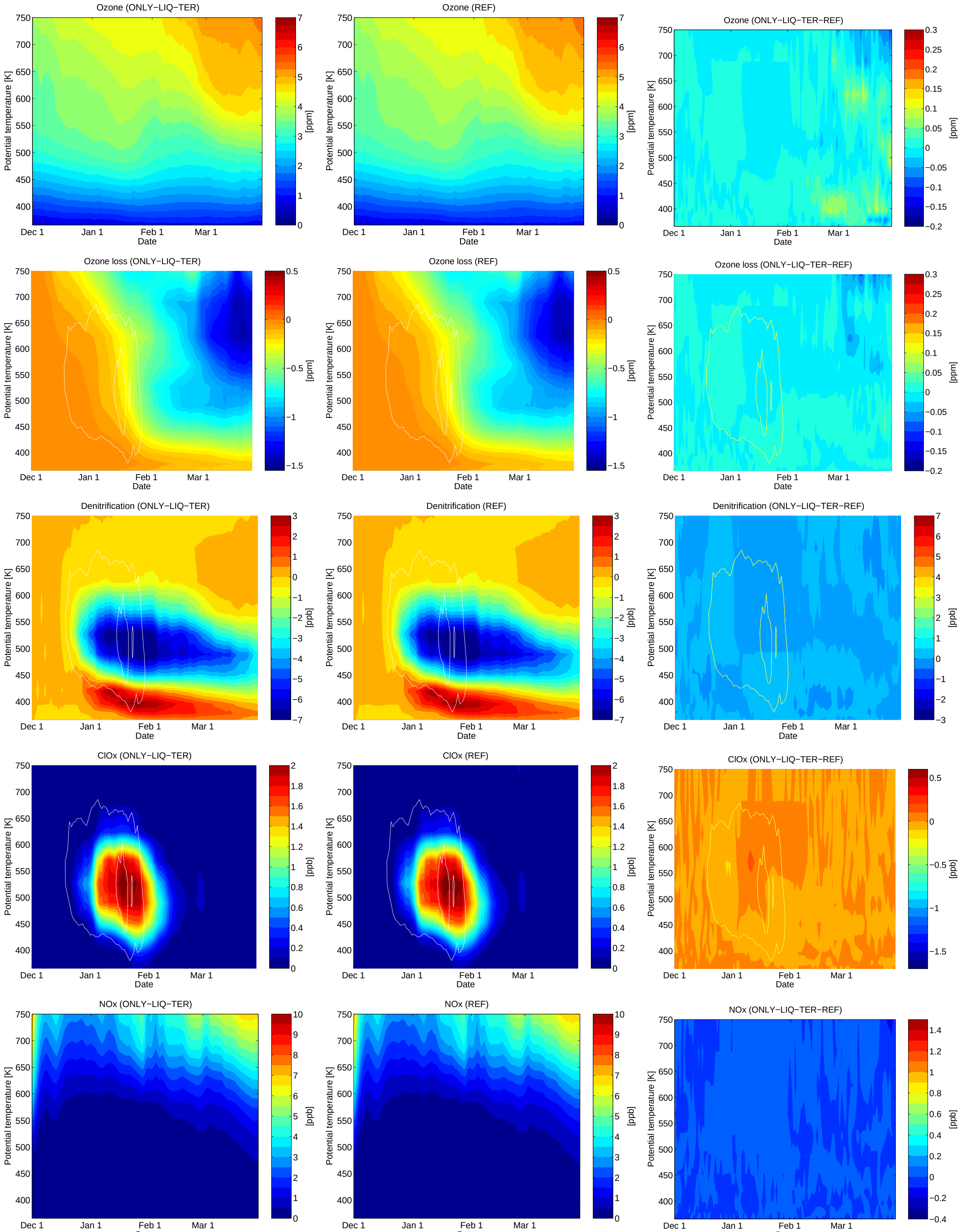

Figure 20: Vortex means as a function of model date and potential temperature inside the vortex boundary according to Nash. Left column: sensitivity run (ONLY-LIQ-TER), middle column: reference run, right column: difference (sensitivity minus reference run). From top to bottom: ozone, ozone loss (difference of ozone to passive tracer), denitrification (difference of NO_y to passive tracer), ClO_x and NO_x. White lines show the time periods where the formation of NAT clouds (outer line) and ice clouds (inner line) was possible inside the vortex.

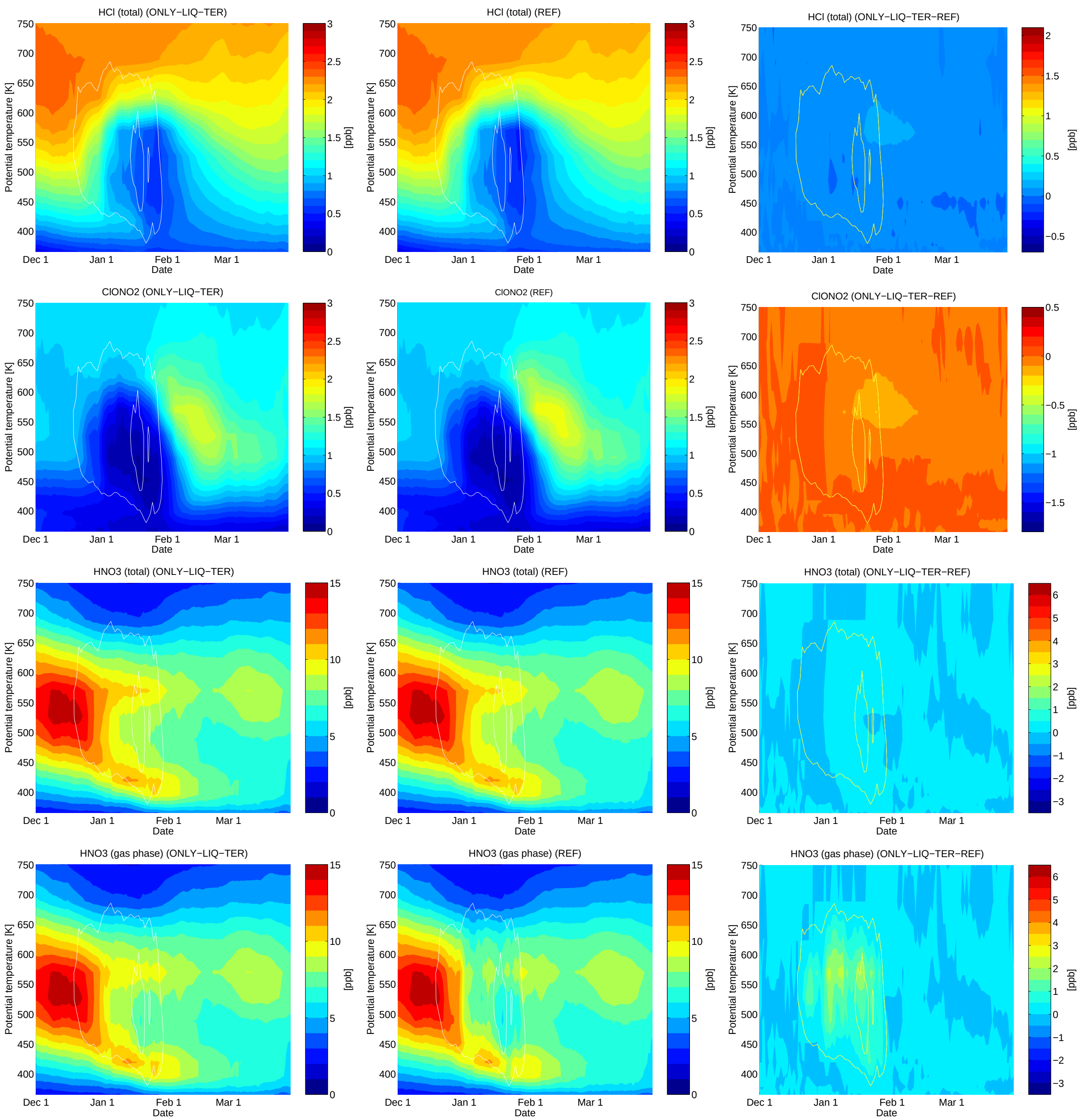

Figure 21: Vortex means as a function of model date and potential temperature inside the vortex boundary according to Nash. Left column: sensitivity run (ONLY-LIQ-TER), middle column: reference run, right column: difference (sensitivity minus reference run). From top to bottom: HCl, $ClONO_2$, HNO_3 (total), HNO_3 (gas phase). White lines show the time periods where the formation of NAT clouds (outer line) and ice clouds (inner line) was possible inside the vortex.

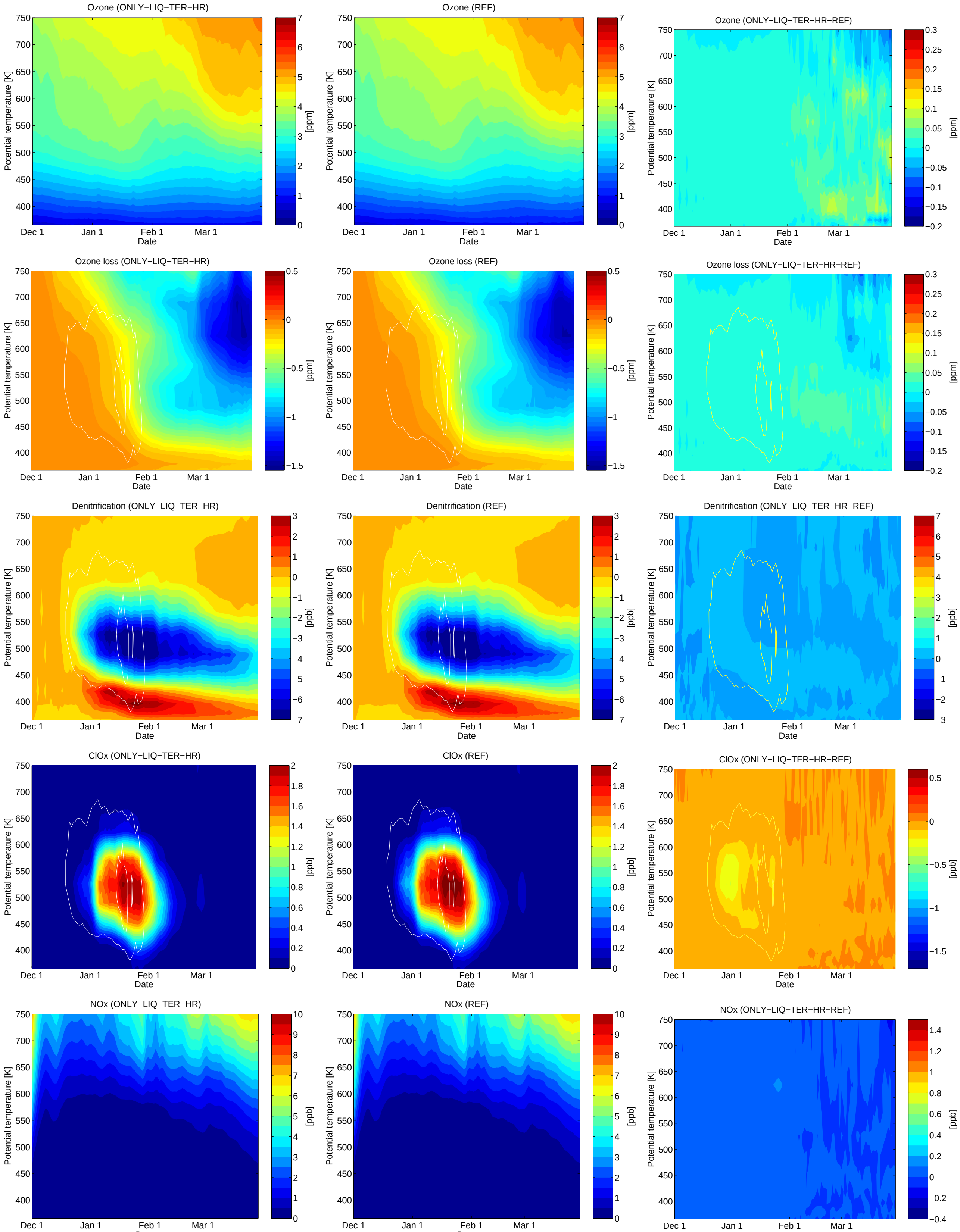

Figure 22: Vortex means as a function of model date and potential temperature inside the vortex boundary according to Nash. Left column: sensitivity run (ONLY-LIQ-TER-HR), middle column: reference run, right column: difference (sensitivity minus reference run). From top to bottom: ozone, ozone loss (difference of ozone to passive tracer), denitrification (difference of NO_y to passive tracer), ClO_x and NO_x. White lines show the time periods where the formation of NAT clouds (outer line) and ice clouds (inner line) was possible inside the vortex.

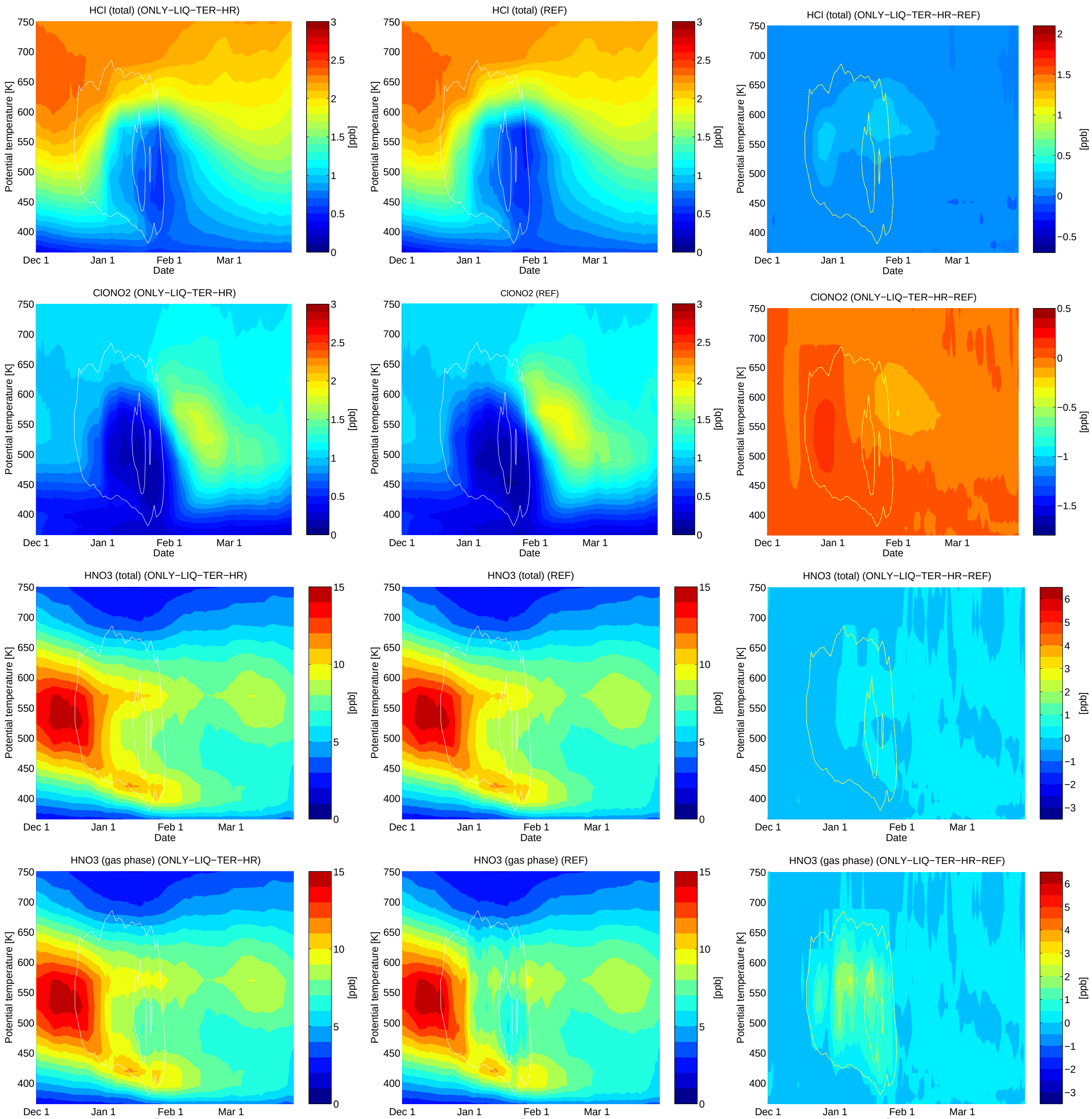

Figure 23: Vortex means as a function of model date and potential temperature inside the vortex boundary according to Nash. Left column: sensitivity run (ONLY-LIQ-TER-HR), middle column: reference run, right column: difference (sensitivity minus reference run). From top to bottom: HCl, $ClONO_2$, HNO_3 (total), HNO_3 (gas phase). White lines show the time periods where the formation of NAT clouds (outer line) and ice clouds (inner line) was possible inside the vortex.

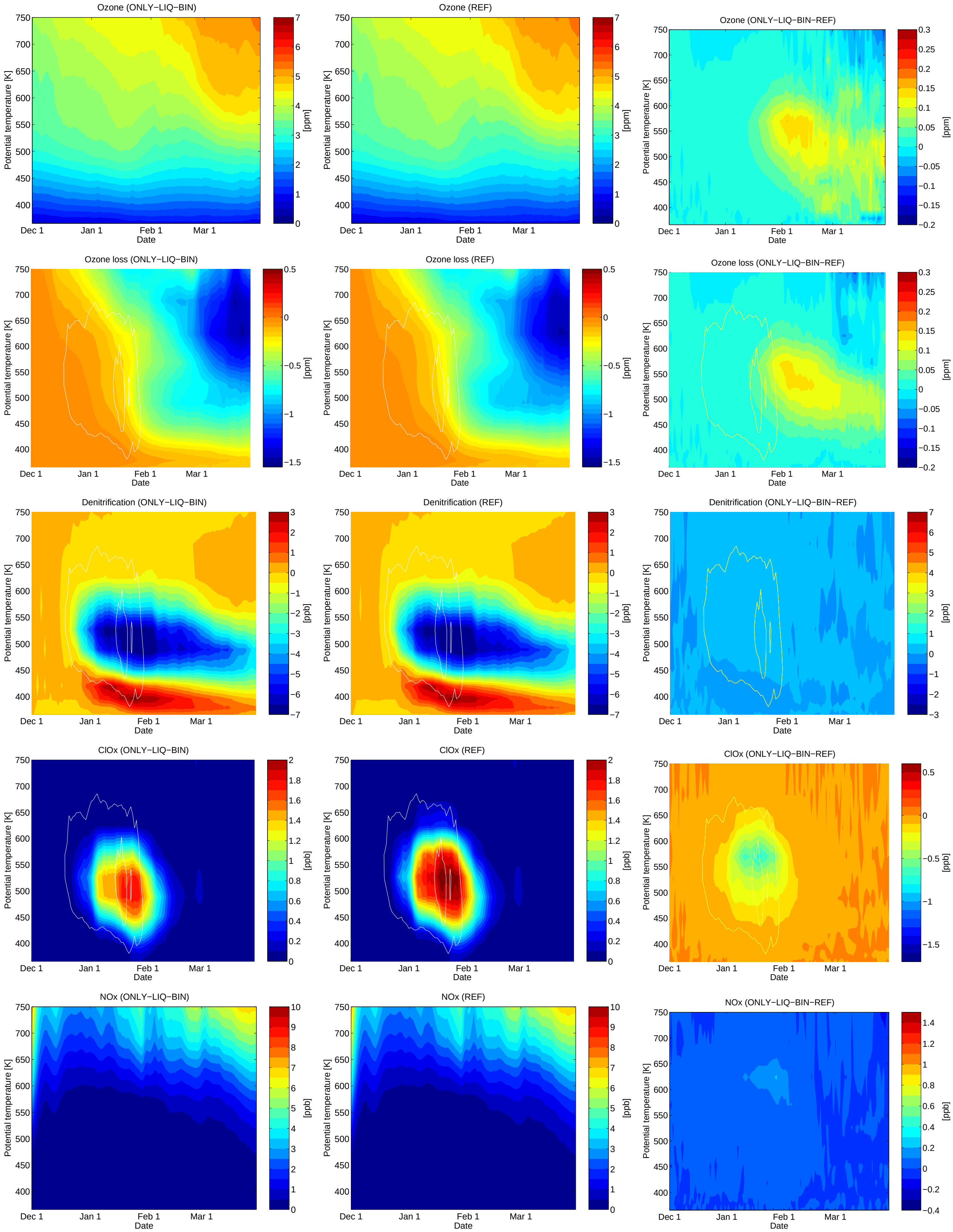

Figure 24: Vortex means as a function of model date and potential temperature inside the vortex boundary according to Nash. Left column: sensitivity run (ONLY-LIQ-BIN), middle column: reference run, right column: difference (sensitivity minus reference run). From top to bottom: ozone, ozone loss (difference of ozone to passive tracer), denitrification (difference of NO_y to passive tracer), ClO_x and NO_x. White lines show the time periods where the formation of NAT clouds (outer line) and ice clouds (inner line) was possible inside the vortex.

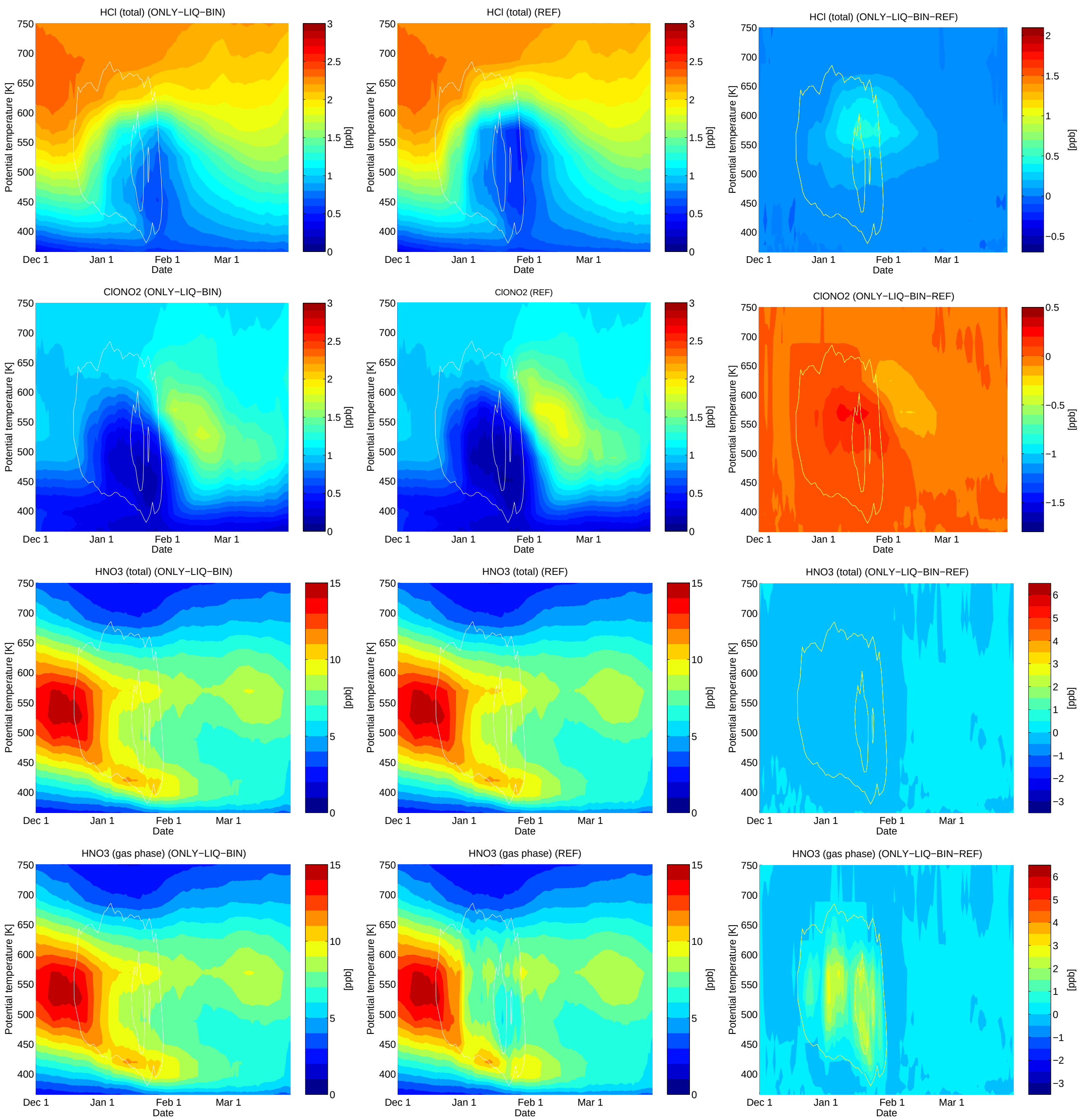

Figure 25: Vortex means as a function of model date and potential temperature inside the vortex boundary according to Nash. Left column: sensitivity run (ONLY-LIQ-BIN), middle column: reference run, right column: difference (sensitivity minus reference run). From top to bottom: HCl, $ClONO_2$, HNO_3 (total), HNO_3 (gas phase). White lines show the time periods where the formation of NAT clouds (outer line) and ice clouds (inner line) was possible inside the vortex.

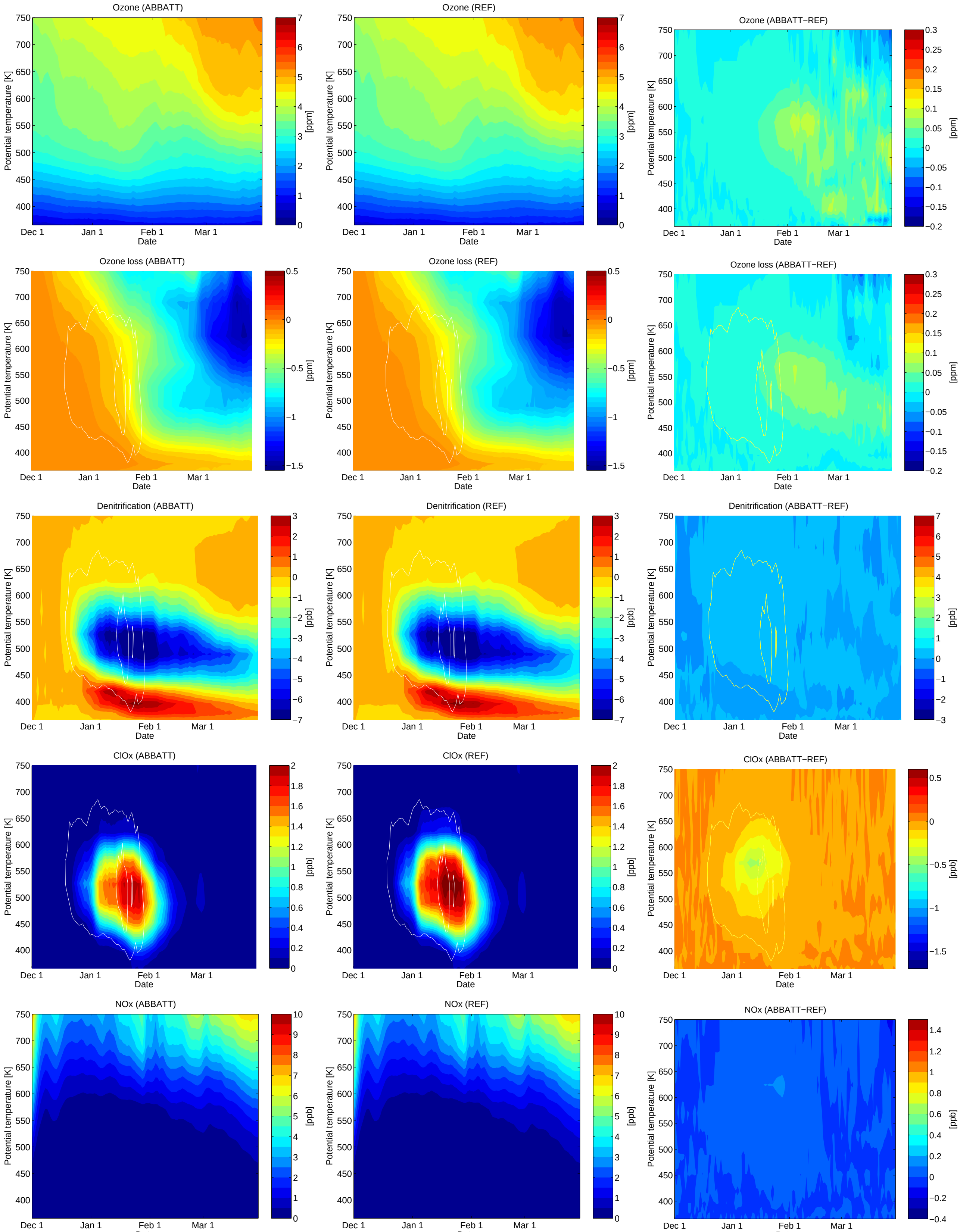

Figure 26: Vortex means as a function of model date and potential temperature inside the vortex boundary according to Nash. Left column: sensitivity run (ABBATT), middle column: reference run, right column: difference (sensitivity minus reference run). From top to bottom: ozone, ozone loss (difference of ozone to passive tracer), denitrification (difference of NO_y to passive tracer), ClO_x and NO_x. White lines show the time periods where the formation of NAT clouds (outer line) and ice clouds (inner line) was possible inside the vortex.

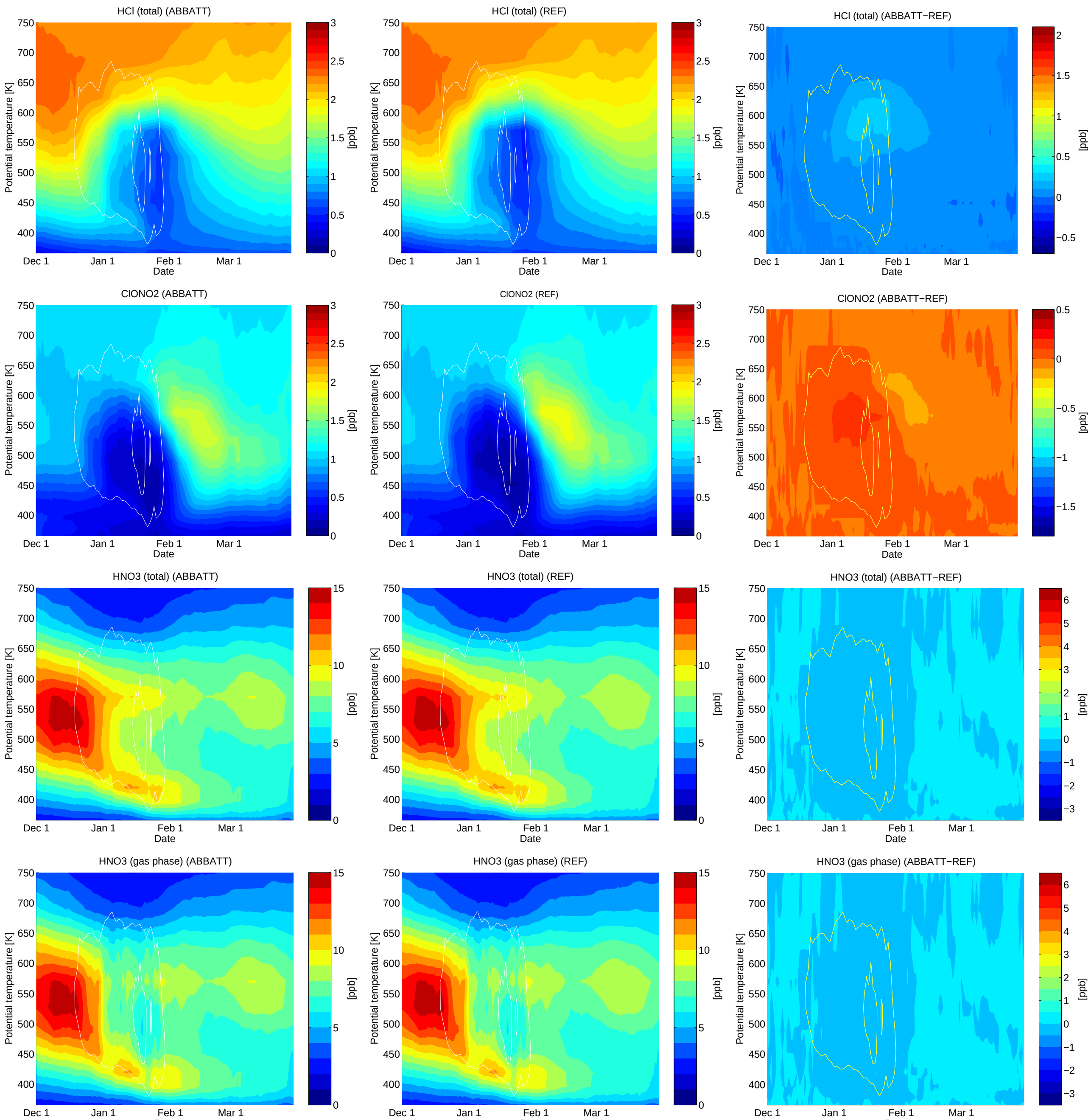

Figure 27: Vortex means as a function of model date and potential temperature inside the vortex boundary according to Nash. Left column: sensitivity run (ABBATT), middle column: reference run, right column: difference (sensitivity minus reference run). From top to bottom: HCl, $ClONO_2$, HNO_3 (total), HNO_3 (gas phase). White lines show the time periods where the formation of NAT clouds (outer line) and ice clouds (inner line) was possible inside the vortex.

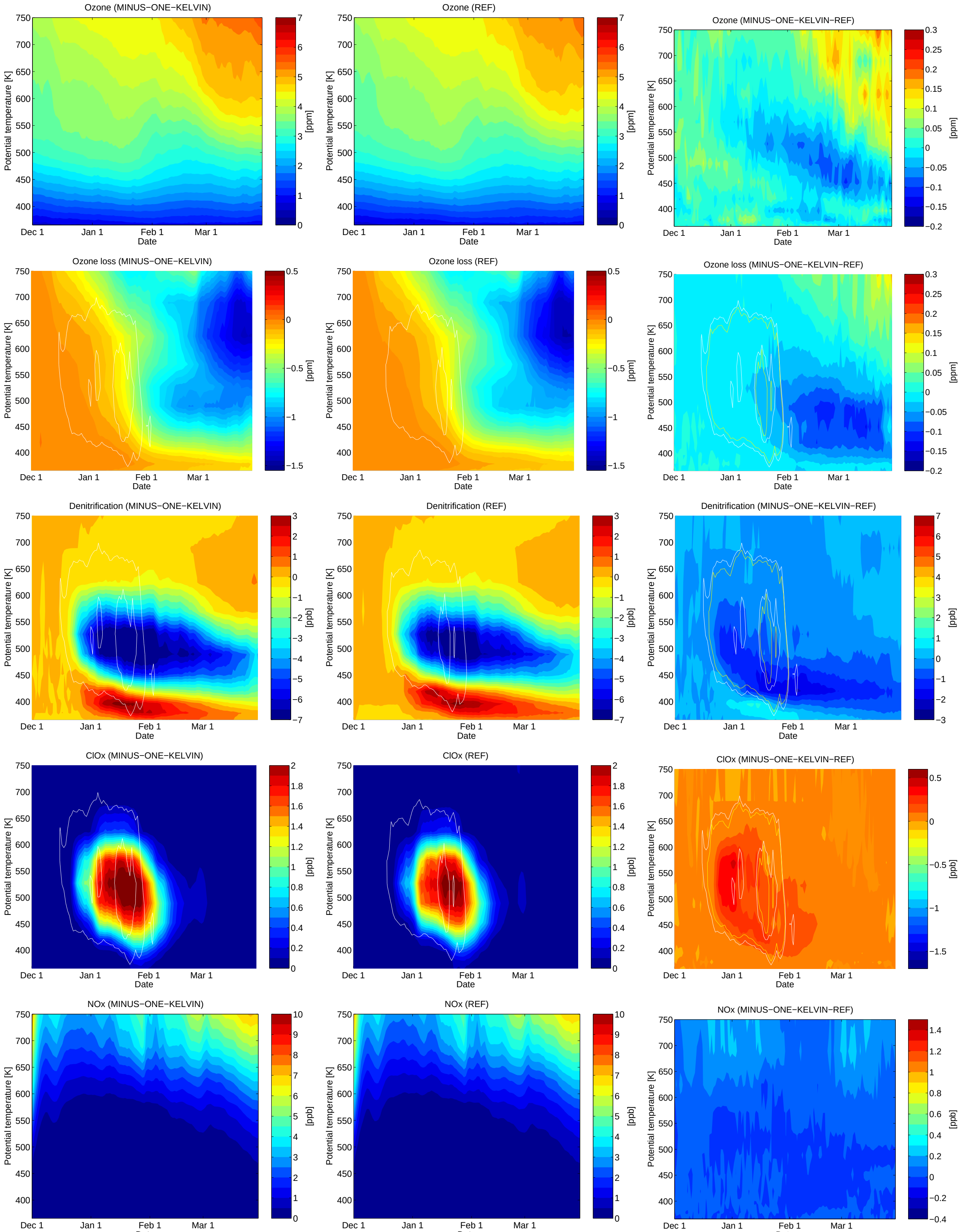

Figure 28: Vortex means as a function of model date and potential temperature inside the vortex boundary according to Nash. Left column: sensitivity run (MINUS-ONE-KELVIN), middle column: reference run, right column: difference (sensitivity minus reference run). From top to bottom: ozone, ozone loss (difference of ozone to passive tracer), denitrification (difference of NO_y to passive tracer), ClO_x and NO_x. White lines show the time periods where the formation of NAT clouds (outer line) and ice clouds (inner line) was possible inside the vortex.

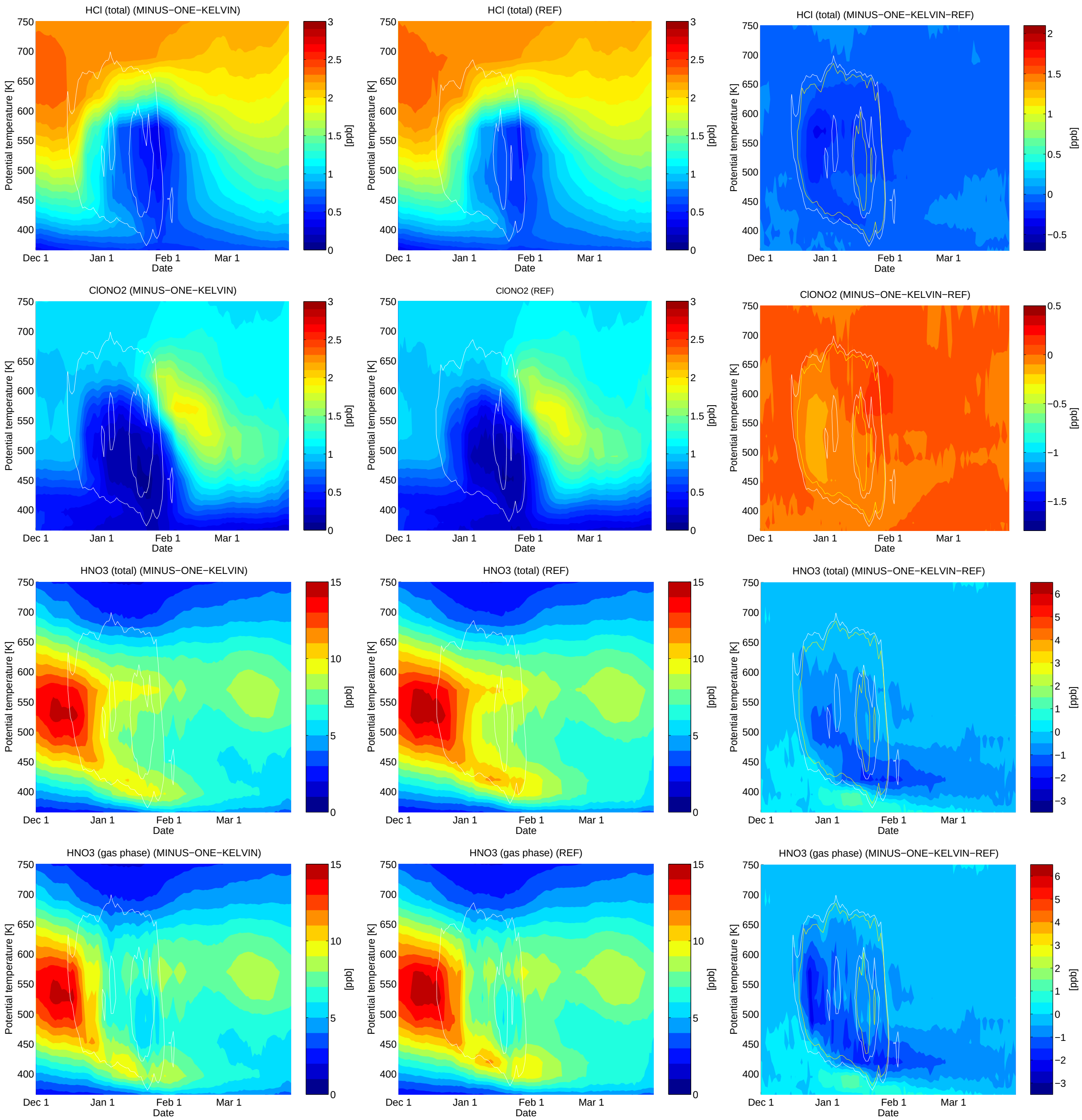

Figure 29: Vortex means as a function of model date and potential temperature inside the vortex boundary according to Nash. Left column: sensitivity run (MINUS-ONE-KELVIN), middle column: reference run, right column: difference (sensitivity minus reference run). From top to bottom: HCl, $ClONO_2$, HNO_3 (total), HNO_3 (gas phase). White lines show the time periods where the formation of NAT clouds (outer line) and ice clouds (inner line) was possible inside the vortex.

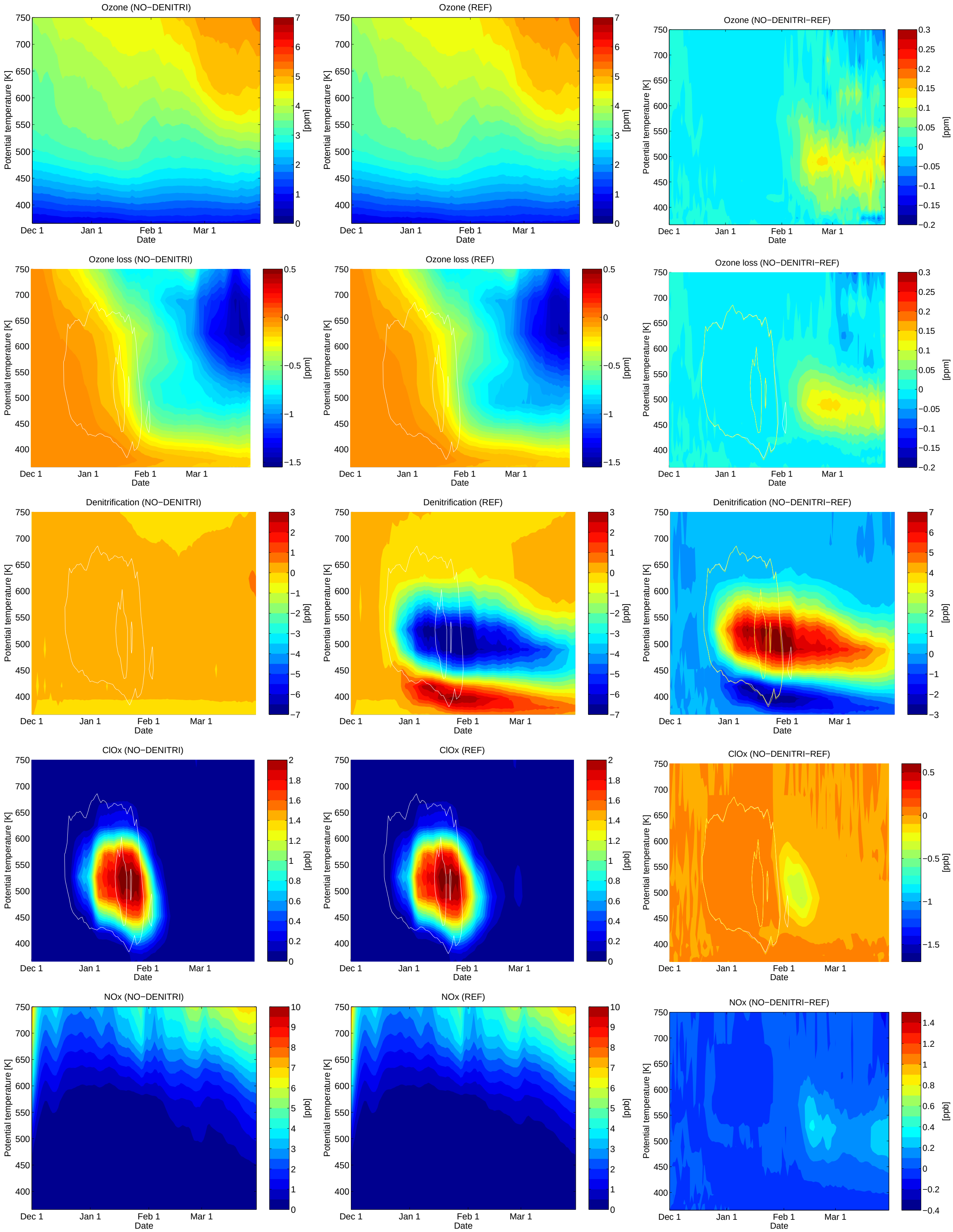

Figure 30: Vortex means as a function of model date and potential temperature inside the vortex boundary according to Nash. Left column: sensitivity run (NO-DENITRI), middle column: reference run, right column: difference (sensitivity minus reference run). From top to bottom: ozone, ozone loss (difference of ozone to passive tracer), denitrification (difference of NO_y to passive tracer), ClO_x and NO_x. White lines show the time periods where the formation of NAT clouds (outer line) and ice clouds (inner line) was possible inside the vortex.

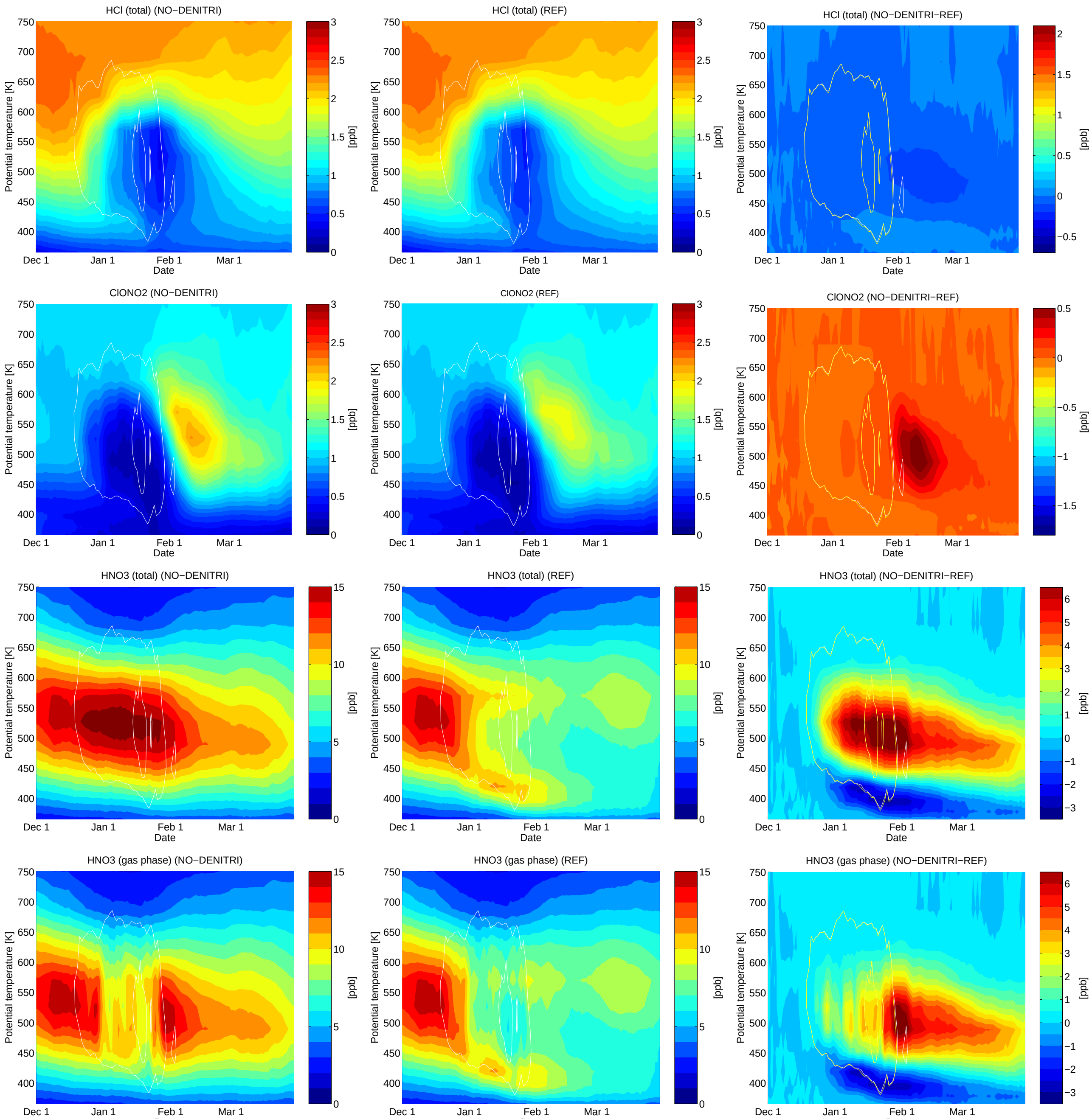

Figure 31: Vortex means as a function of model date and potential temperature inside the vortex boundary according to Nash. Left column: sensitivity run (NO-DENITRI), middle column: reference run, right column: difference (sensitivity minus reference run). From top to bottom: HCl, $ClONO_2$, HNO_3 (total), HNO_3 (gas phase). White lines show the time periods where the formation of NAT clouds (outer line) and ice clouds (inner line) was possible inside the vortex.

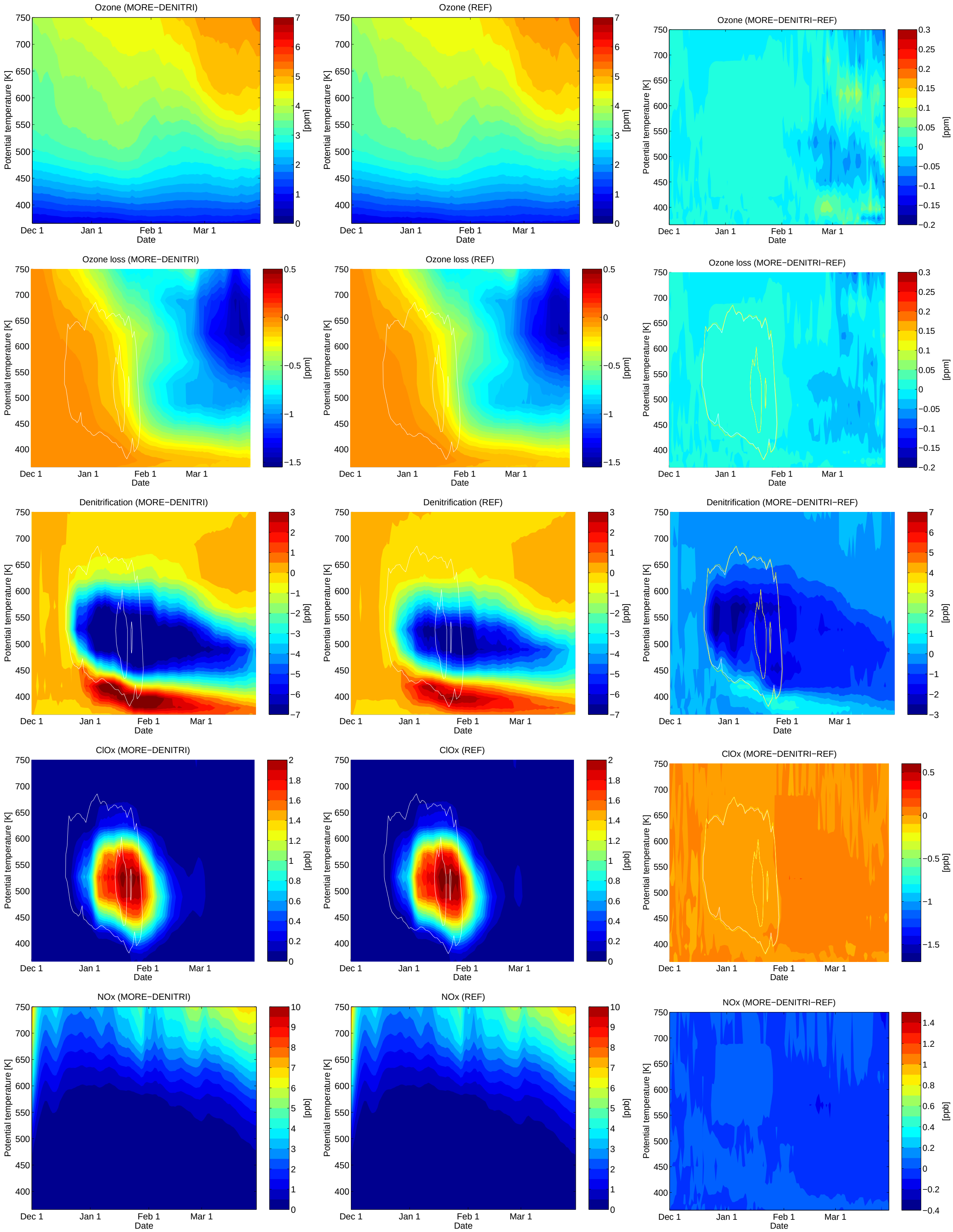

Figure 32: Vortex means as a function of model date and potential temperature inside the vortex boundary according to Nash. Left column: sensitivity run (MORE-DENITRI), middle column: reference run, right column: difference (sensitivity minus reference run). From top to bottom: ozone, ozone loss (difference of ozone to passive tracer), denitrification (difference of NO_y to passive tracer), ClO_x and NO_x. White lines show the time periods where the formation of NAT clouds (outer line) and ice clouds (inner line) was possible inside the vortex.

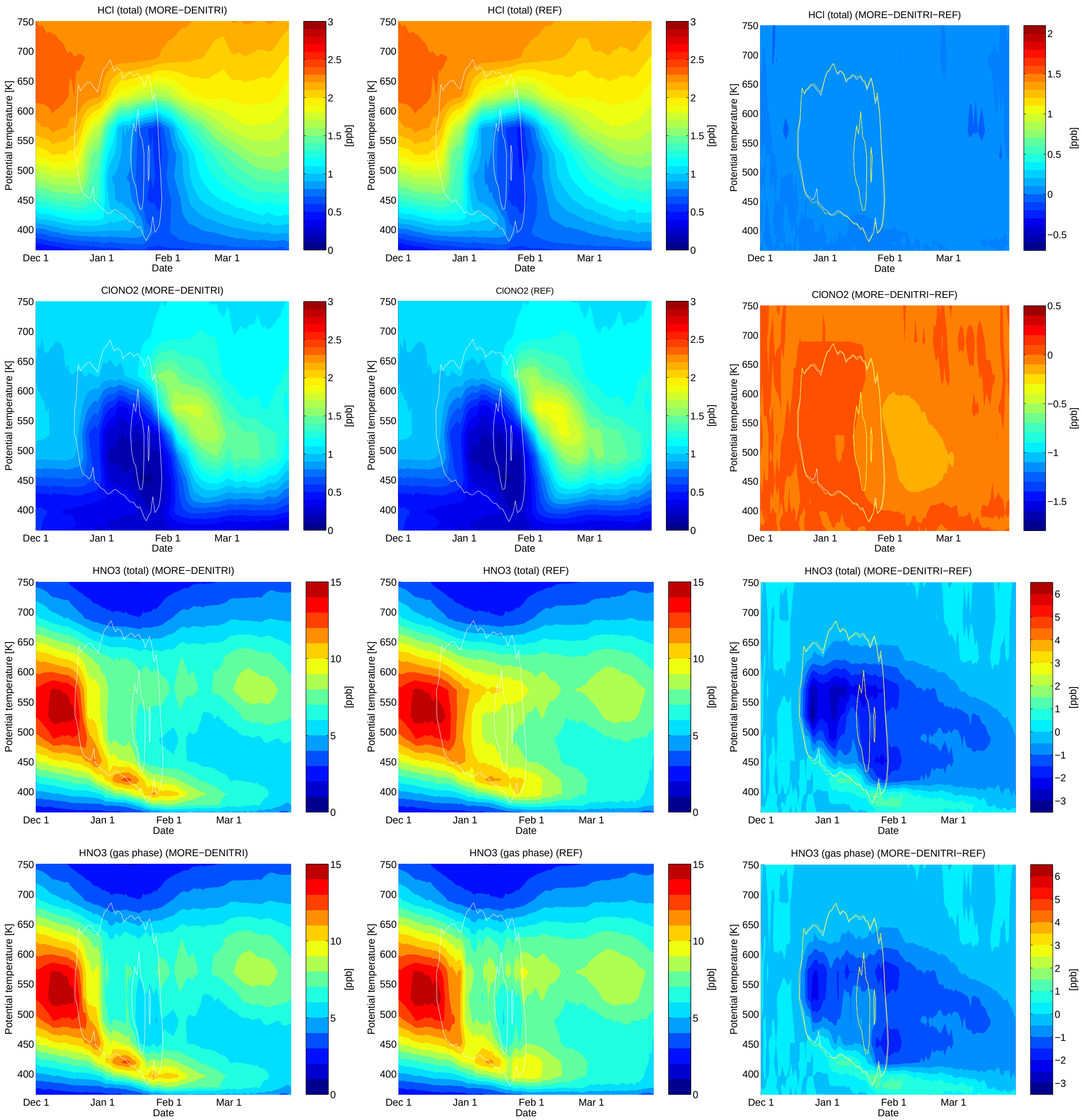

Figure 33: Vortex means as a function of model date and potential temperature inside the vortex boundary according to Nash. Left column: sensitivity run (MORE-DENITRI), middle column: reference run, right column: difference (sensitivity minus reference run). From top to bottom: HCl, $ClONO_2$, HNO_3 (total), HNO_3 (gas phase). White lines show the time periods where the formation of NAT clouds (outer line) and ice clouds (inner line) was possible inside the vortex.

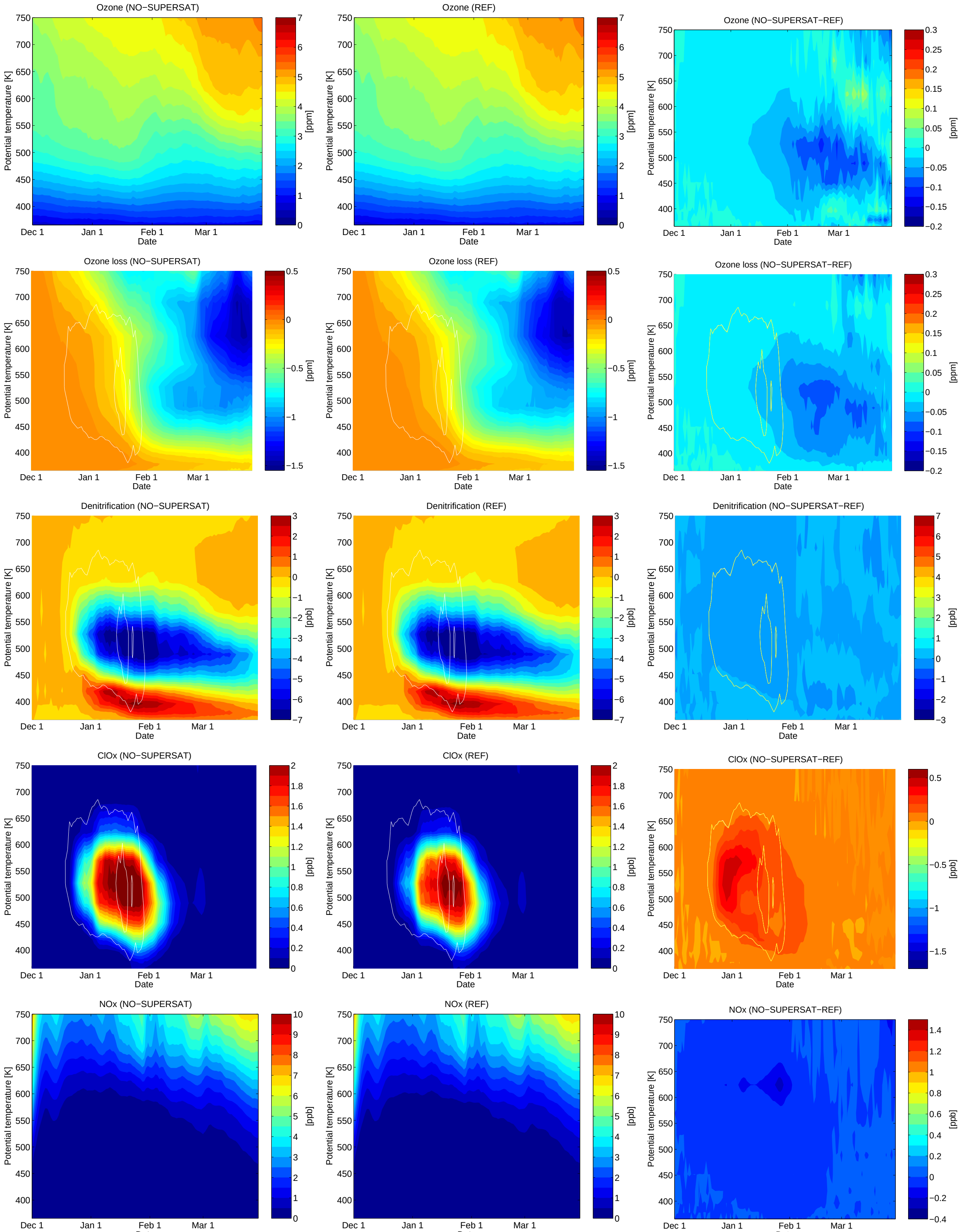

Figure 34: Vortex means as a function of model date and potential temperature inside the vortex boundary according to Nash. Left column: sensitivity run (NO-SUPERSAT), middle column: reference run, right column: difference (sensitivity minus reference run). From top to bottom: ozone, ozone loss (difference of ozone to passive tracer), denitrification (difference of NO_y to passive tracer), ClO_x and NO_x. White lines show the time periods where the formation of NAT clouds (outer line) and ice clouds (inner line) was possible inside the vortex.

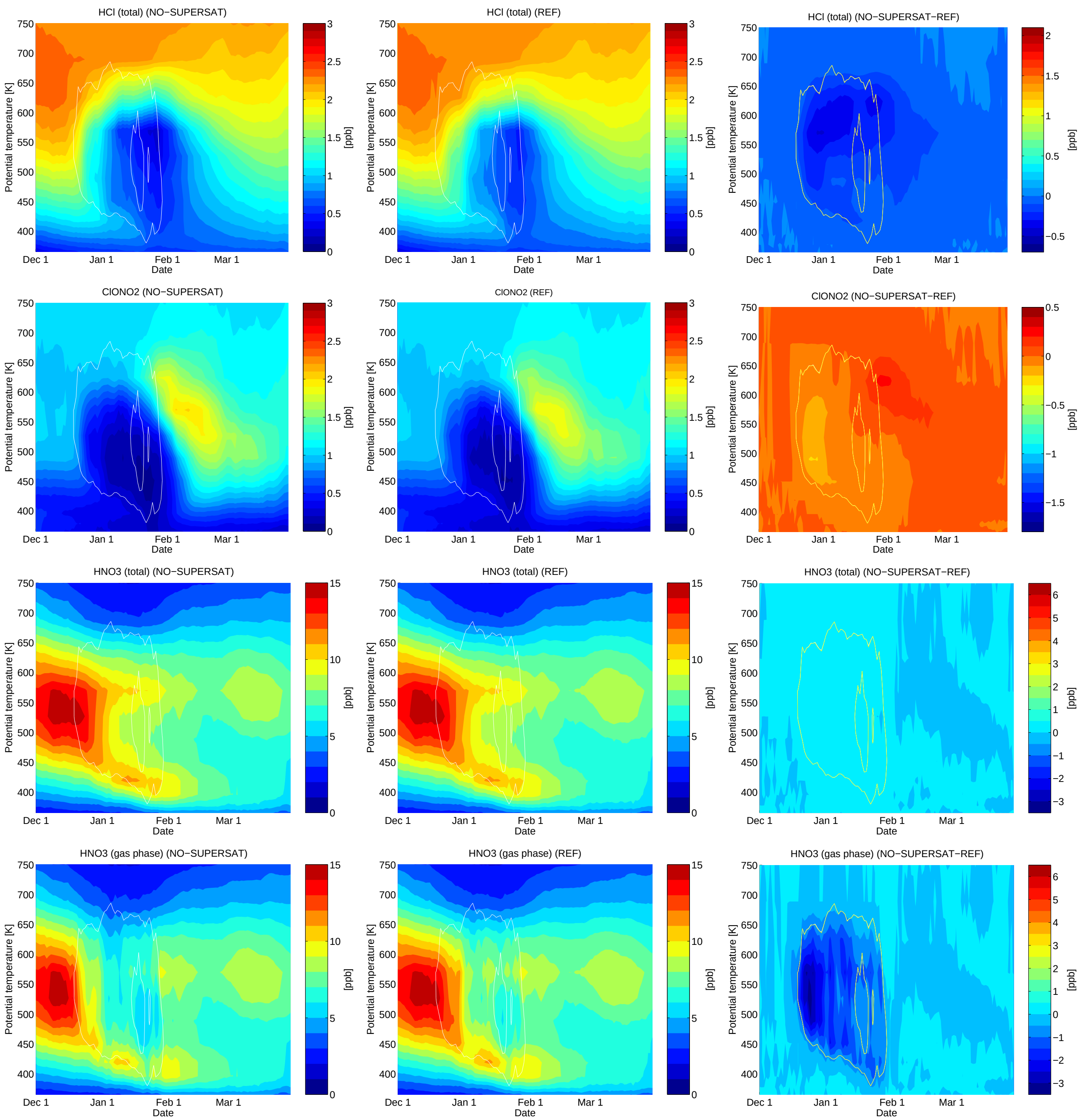

Figure 35: Vortex means as a function of model date and potential temperature inside the vortex boundary according to Nash. Left column: sensitivity run (NO-SUPERSAT), middle column: reference run, right column: difference (sensitivity minus reference run). From top to bottom: HCl, $ClONO_2$, HNO_3 (total), HNO_3 (gas phase). White lines show the time periods where the formation of NAT clouds (outer line) and ice clouds (inner line) was possible inside the vortex.

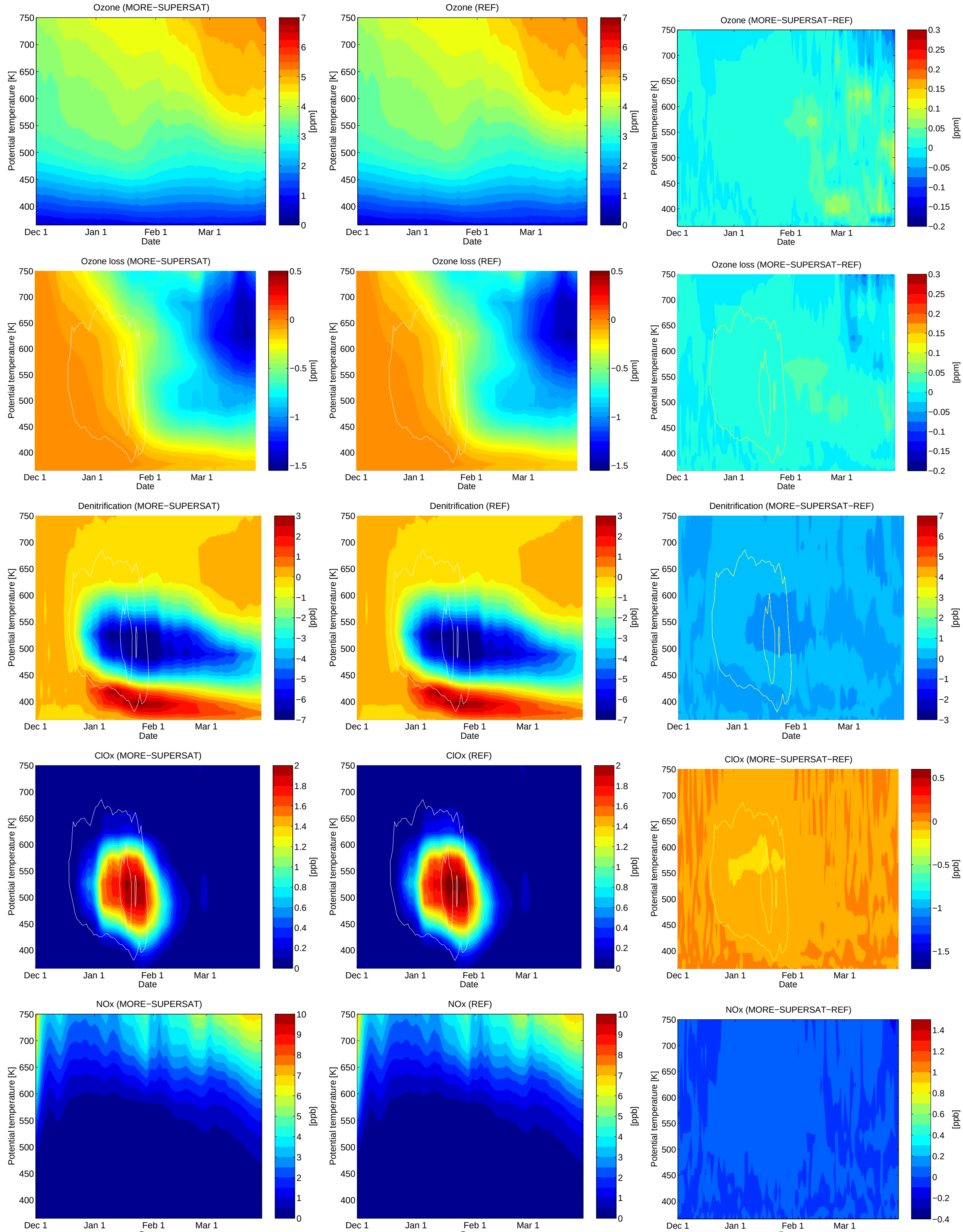

Figure 36: Vortex means as a function of model date and potential temperature inside the vortex boundary according to Nash. Left column: sensitivity run (MORE-SUPERSAT), middle column: reference run, right column: difference (sensitivity minus reference run). From top to bottom: ozone, ozone loss (difference of ozone to passive tracer), denitrification (difference of NO_y to passive tracer), ClO_x and NO_x. White lines show the time periods where the formation of NAT clouds (outer line) and ice clouds (inner line) was possible inside the vortex.

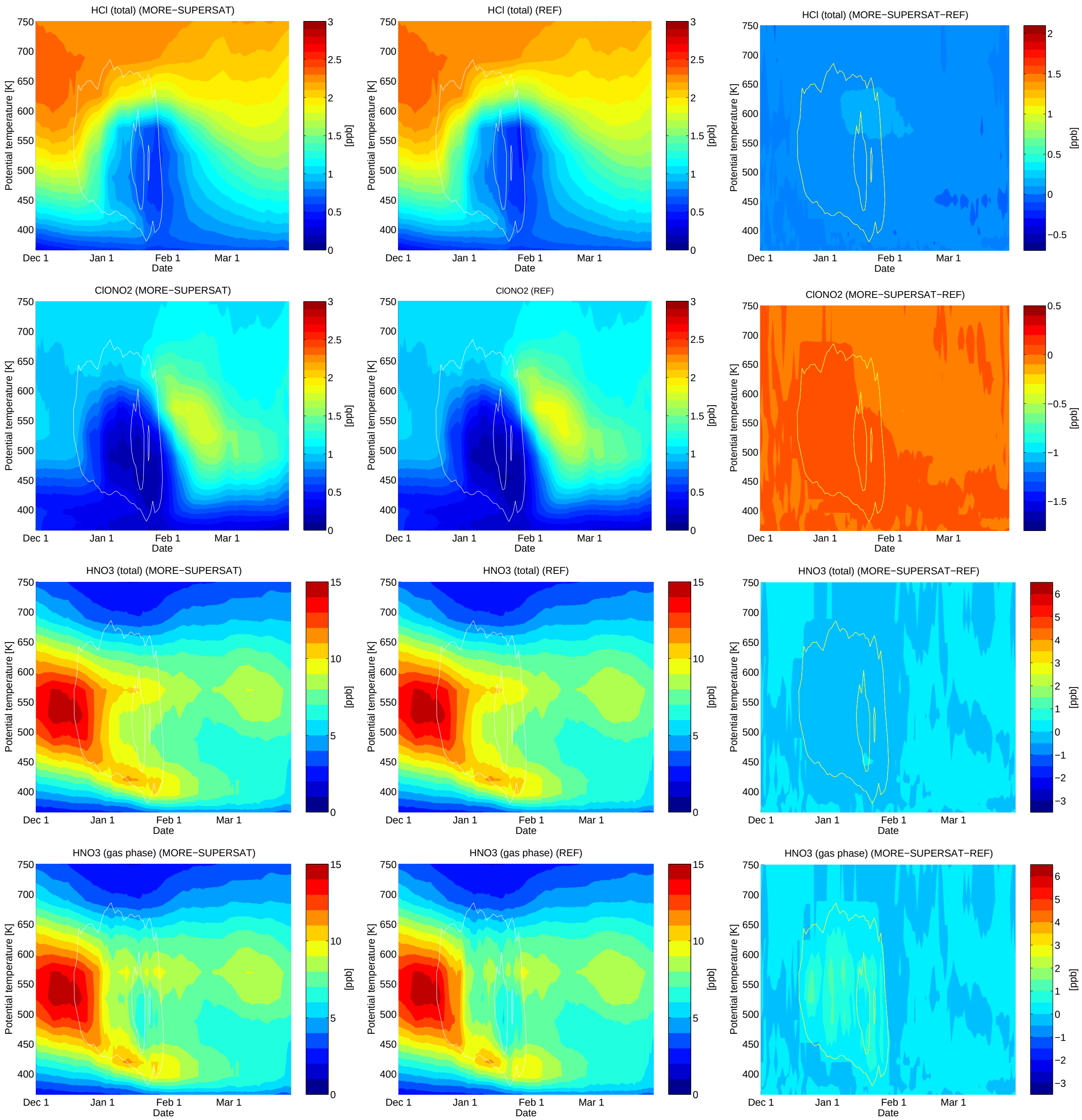

Figure 37: Vortex means as a function of model date and potential temperature inside the vortex boundary according to Nash. Left column: sensitivity run (MORE-SUPERSAT), middle column: reference run, right column: difference (sensitivity minus reference run). From top to bottom: HCl, $ClONO_2$, HNO_3 (total), HNO_3 (gas phase). White lines show the time periods where the formation of NAT clouds (outer line) and ice clouds (inner line) was possible inside the vortex.

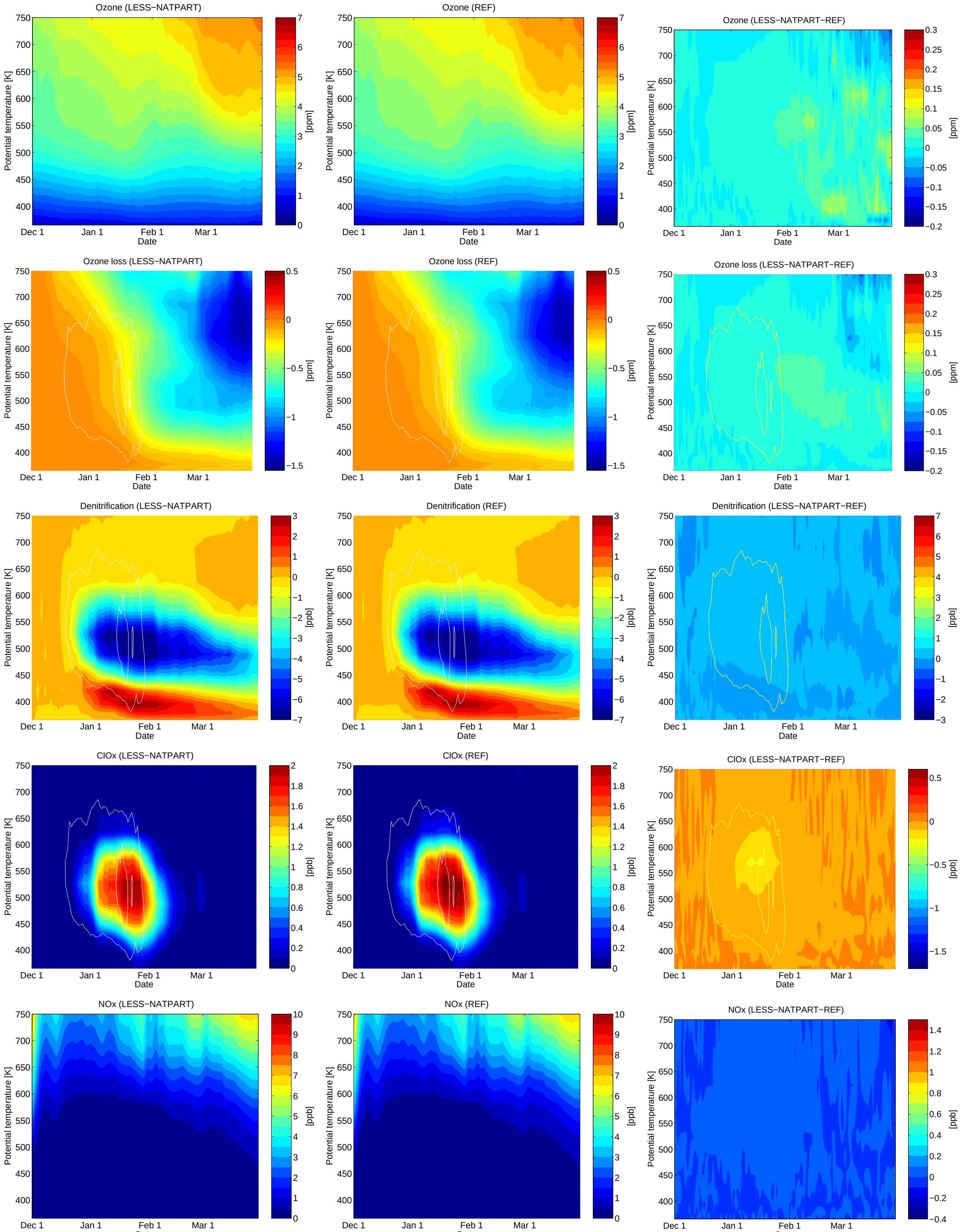

Figure 38: Vortex means as a function of model date and potential temperature inside the vortex boundary according to Nash. Left column: sensitivity run (LESS-NATPART), middle column: reference run, right column: difference (sensitivity minus reference run). From top to bottom: ozone, ozone loss (difference of ozone to passive tracer), denitrification (difference of NO_y to passive tracer), ClO_x and NO_x. White lines show the time periods where the formation of NAT clouds (outer line) and ice clouds (inner line) was possible inside the vortex.

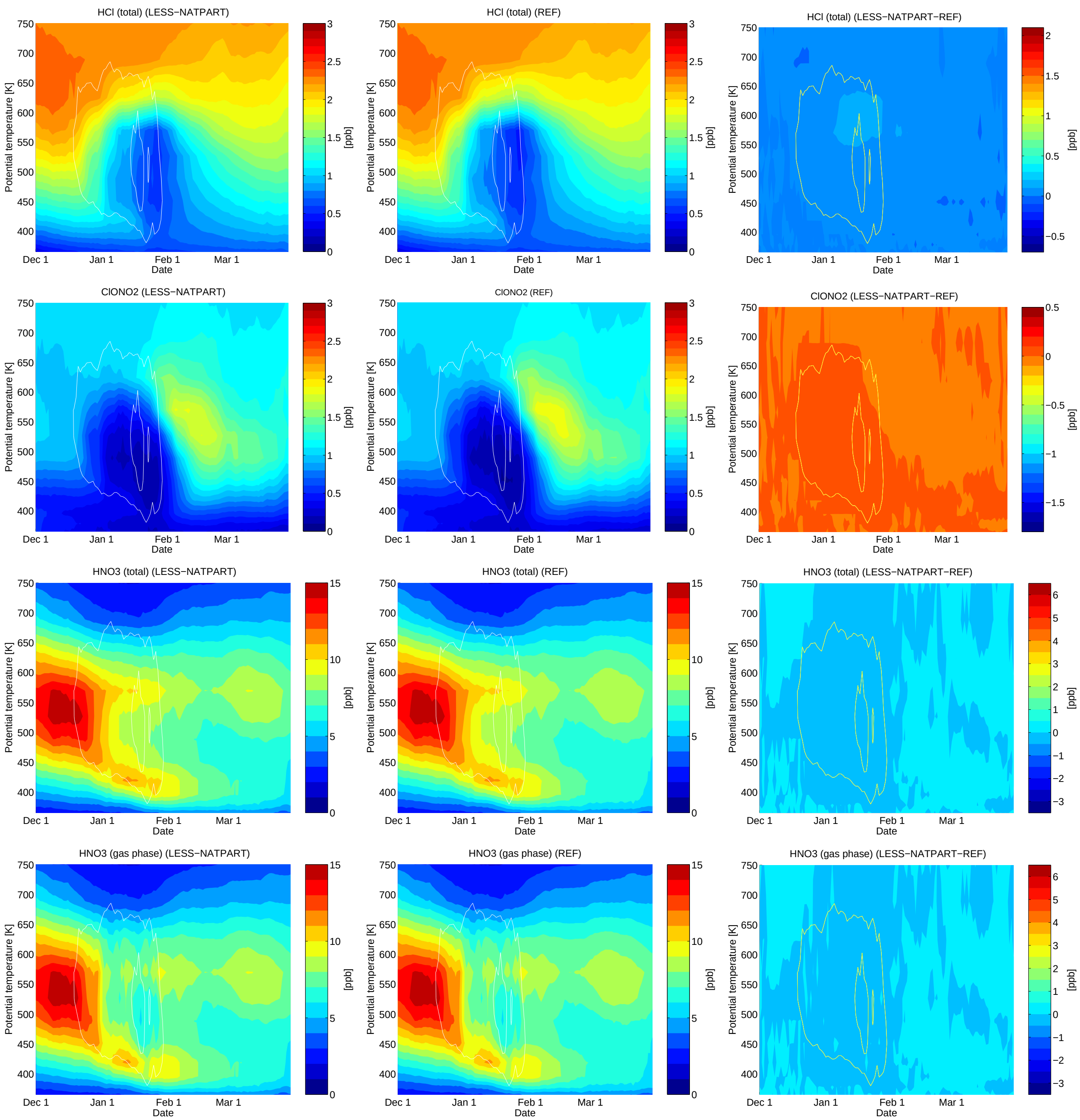

Figure 39: Vortex means as a function of model date and potential temperature inside the vortex boundary according to Nash. Left column: sensitivity run (LESS-NATPART), middle column: reference run, right column: difference (sensitivity minus reference run). From top to bottom: HCl, $ClONO_2$, HNO_3 (total), HNO_3 (gas phase). White lines show the time periods where the formation of NAT clouds (outer line) and ice clouds (inner line) was possible inside the vortex.

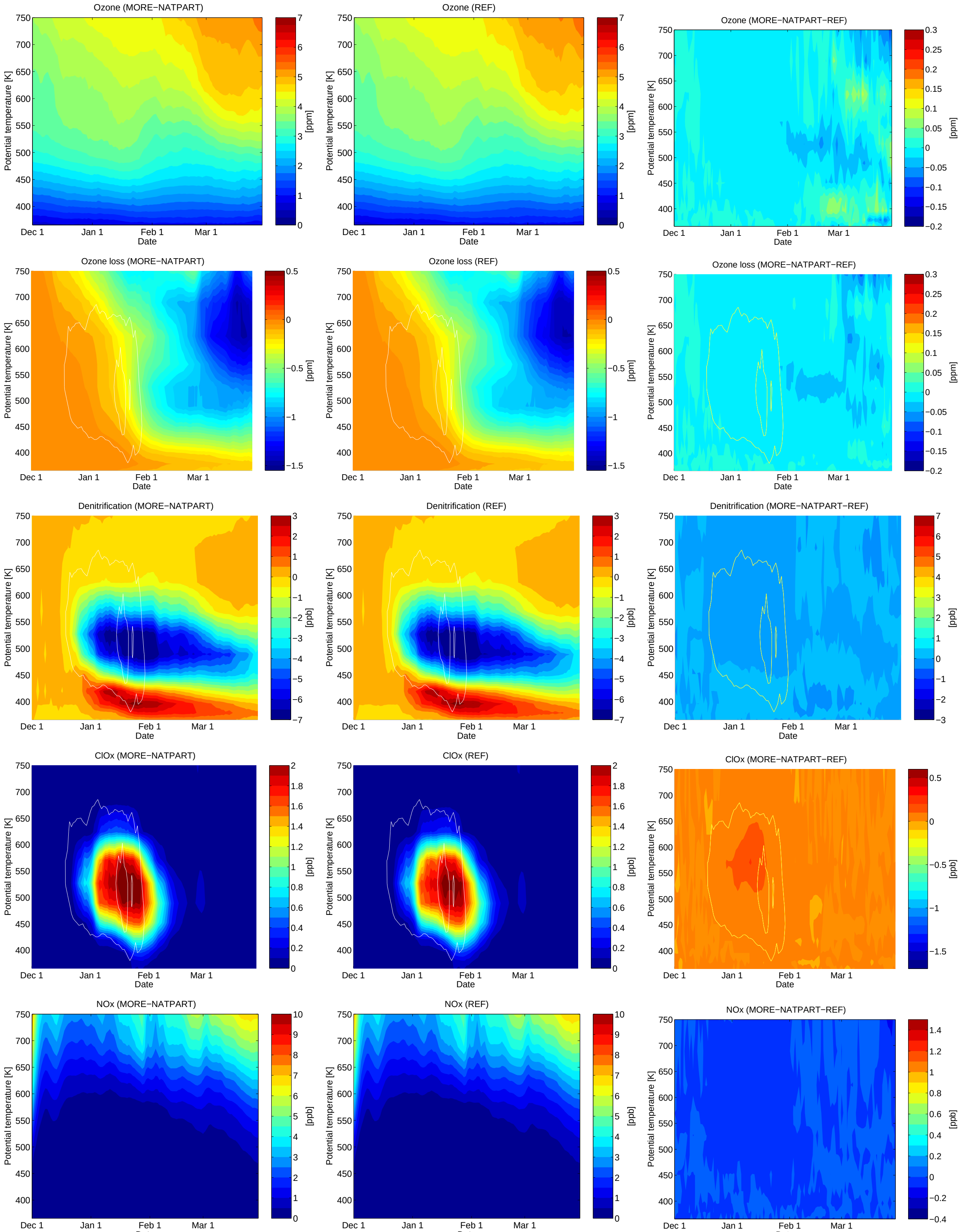

Figure 40: Vortex means as a function of model date and potential temperature inside the vortex boundary according to Nash. Left column: sensitivity run (MORE-NATPART), middle column: reference run, right column: difference (sensitivity minus reference run). From top to bottom: ozone, ozone loss (difference of ozone to passive tracer), denitrification (difference of NO_y to passive tracer), ClO_x and NO_x. White lines show the time periods where the formation of NAT clouds (outer line) and ice clouds (inner line) was possible inside the vortex.

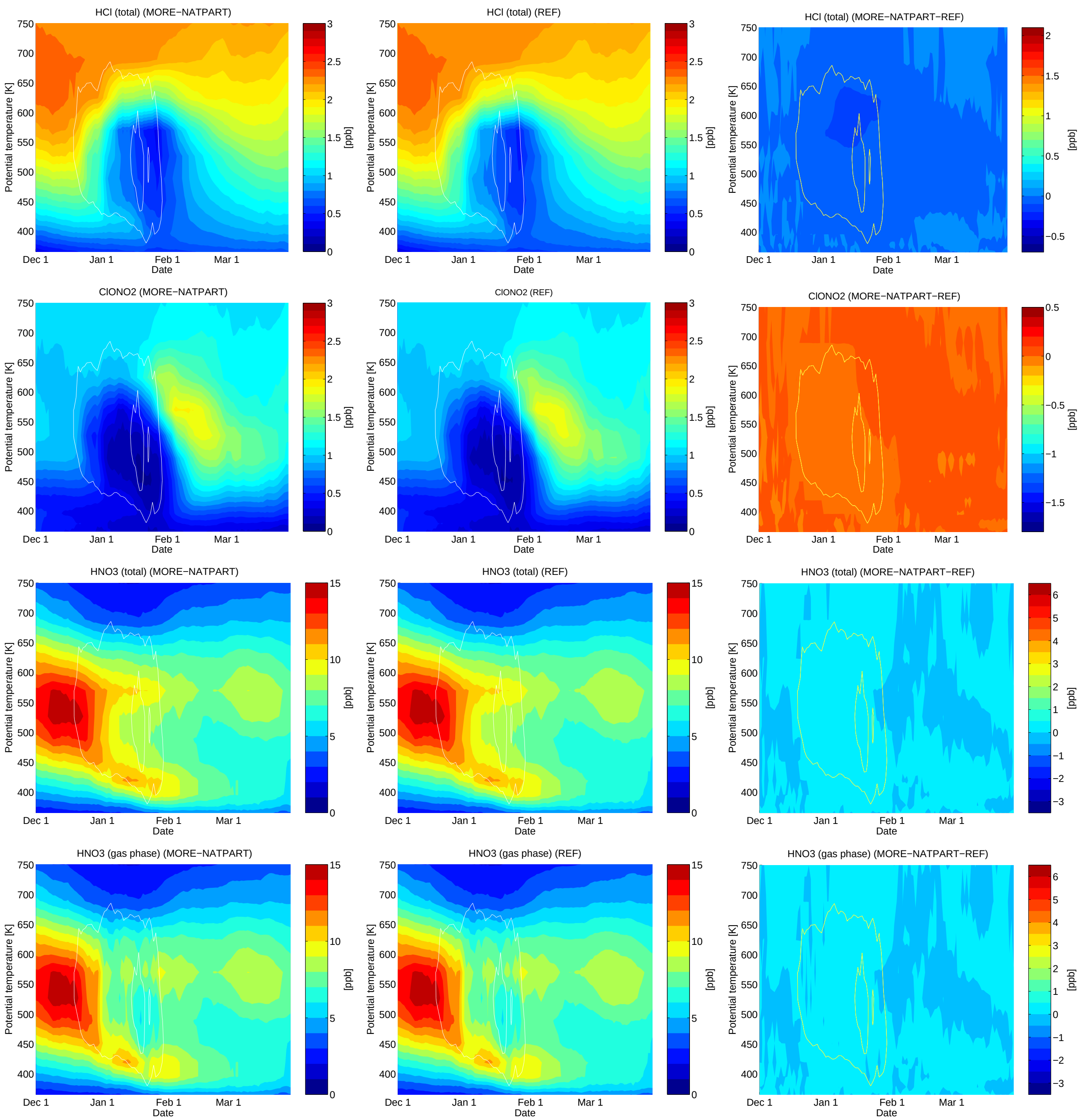

Figure 41: Vortex means as a function of model date and potential temperature inside the vortex boundary according to Nash. Left column: sensitivity run (MORE-NATPART), middle column: reference run, right column: difference (sensitivity minus reference run). From top to bottom: HCl, $ClONO_2$, HNO_3 (total), HNO_3 (gas phase). White lines show the time periods where the formation of NAT clouds (outer line) and ice clouds (inner line) was possible inside the vortex.